Design and Development of Aerial Fertilizer Spreader for Improved Efficiency

Author

MUHAMMAD SHOAIB

00000273718

Supervisor

Dr. IMRAN AKHTAR

DEPARTMENT OF MECHANICAL ENGINEERING

COLLEGE OF ELECTRICAL & MECHANICAL ENGINEERING

NATIONAL UNIVERSITY OF SCIENCES AND TECHNOLOGY

ISLAMABAD

AUG, 2022

Design and Development of Aerial Fertilizer Spreader for Improved Efficiency

Author

MUHAMMAD SHOAIB

00000273718

A thesis submitted in partial fulfillment of the requirements for the degree of

MS Mechanical Engineering

Thesis Supervisor:

Dr. IMRAN AKHTAR

DEPARTMENT OF MECHANICAL ENGINEERING

COLLEGE OF ELECTRICAL & MECHANICAL ENGINEERING

NATIONAL UNIVERSITY OF SCIENCES AND TECHNOLOGY,

ISLAMABAD

AUG, 2022

Declaration

I certify that this research work titled "*Design and Development of Aerial Fertilizer Spreader for Improved Efficiency"* is my own work. The work has not been presented elsewhere for assessment. The material that has been used from other sources it has been properly acknowledged / referred.

_____

Muhammad Shoaib

00000273718

MS-2018 Mechanical Engineering

College of Electrical & Mechanical Engineering

National University of Sciences and Technology, Islamabad

Language Correctness Certificate

This thesis has been read by an English expert and is free of typing, syntax, semantic, grammatical and spelling mistakes. Thesis is also according to the format given by the university.

Muhammad Shoaib

00000273718
MS-2018 Mechanical Engineering
College of Electrical & Mechanical Engineering
National University of Sciences and Technology, Islamabad

Dr. Imran Akhtar

Assistant Professor
Department of Mechanical Engineering College of Electrical & Mechanical Engineering National University of Sciences and Technology, Islamabad

Copyright Statement

Acknowledgements

All praises, hymns and countless thanks to **ALMIGHTY ALLAH**, the most Gracious, the most Merciful who granted us the strength to perform to the utmost of my abilities and with Whose will all of this was possible. Millions of Darood-o-Salam for **HAZRAT MUHAMMAD** (S.A.W.W.), who is forever a model of guidance and knowledge for humanity as a whole.

I deem it profound honor to express the depth of our gratitude to my Thesis Supervisor **Dr. Imran Akhtar** for accommodating me, with his expertise and knowledge, at every step and turn of the whole ordeal. Despite his busy routine and having his hands full, he took me up, and actively guided and motivated me regarding everything in the thesis with his creative ideas.

I would like to extend my deep appreciation to **Dr. Imran Akhtar**, the **Head of Department** of the Mechanical Department, whose deep insight and understanding of my situation made my thesis possible. He has always provided me with an inspiring attitude and exceptional guidance.

I am greatly indebted to my **friends and family**, especially **Father** who helped me at every step of this process, for their love support and countless prayers.

Dedicated to my exceptional parents and elder brother whose tremendous support and cooperation led me to this wonderful accomplishment

Abstract

Crop production all over the world has been increased dramatically after the production of synthetic fertilizers. Population of the world has been increasing exponentially, putting pressure on limited resources. Now a days, the major concern is the environment. Under and overdose application of fertilizers and pesticides cause damage not only to the crop but also effects the environment. The spread ability and uniformity of the spreader pattern has become significant subject in this age of agricultural engineering.

In the first phase, design and development is completed using solidworks software at Robot Design and Development Lab, NUST. In the second phase, mathematical model is developed to predict the behavior of particle ejected from unmanned aerial fertilizer spreader (UAFS) and a computer program is developed to simulate the particle trajectory and particle distribution. The unmanned aerial fertilizer spreader speed, particle size, density and the atmospheric wind are found to have significant effect on the deposition uniformity and pattern width. The height of unmanned aerial fertilizer also impacts spreading width.

To analyze the actual deposition pattern,field tests are performed. Field tests are found to be associated with high degree of uncertainty in term of variable inputs. Using kinematic equations we have determined the various factors, such as the optimize length of impeller 155mm, optimize angle is between 25 to 30 degrees, optimize RPM 425 and optimize height of (UAFS) is 2 m from crop height, physical parameter such as average fertilizer particle diameter is 2 mm and bulk density is 2000 kg/m^3.

The model is having potential in predicting the trends in change of deposition pattern shape and size with changes in variables like particle properties, unmanned aerial fertilizer speed, altitude and wind speed.

Keywords: Design and development, kinematic equation, AFS, fertilizer and RPM

Table of Contents

List of Figures

List of Tables

Chapter 1 Introduction

1.1 Motivation and Background

Agriculture is the largest labor consuming sector in Pakistan. Pakistan is the second biggest country in South Asia in terms of agriculture area and ranking in the world is 36th.The over-all landscape area of Pakistan is 79.6 million ha, out of which 22 million hector are used for crop production. In Pakistan 86% farmer are small land holding (less than 5 hector) and 5 % are greater than 20 ha [1]. Contribution of agriculture in domestic GDP is continuously increasing. It has covered 37.4% labor of the country and its share in national GDP is 22.7%. [2]. In Pakistan, crop area is large but from production point of view it is far away from developed counties. It is found that due to usage of traditional agricultural methods farmers are unable to gain more crop yield. There is huge demand of development of Engineering systems to modernize agriculture sector and compensate these drawbacks. It is an established fact that, by employing modern systems such as drip irrigation, drone technology and laser leveling, the yield can be increased multiple times which can revolutionize Pakistan’s economy. For this purpose it needs modern agriculture equipment in the field of agriculture [3].

Russia and Ukraine are major suppliers of wheat, pulses, and oilseeds to Pakistan. Russian and Ukrainian imports made up 77.3 percent of the nation's total imports of wheat, 19.3 percent of its total imports of pulses, and 10.4 percent of its total imports of oilseeds last year. Although Pakistan is not primarily dependent on these two nations for fossil fuels and fertilizers, it is anticipated to be hardest hit by rising fertilizer and energy prices globally. Pakistan's goal of producing 28.90 million metric tonnes (MMT) of wheat for the 2021–22 season was missed because of high fertilizer costs and drought in several regions of the nation. Therefore, 3.0 MMT of wheat imports would probably be required by Pakistan over the coming few months. Wheat prices are burgeoning and the conflict between Russia and Ukraine has contributed a sharp rise in these prices. The on-going floods, unstable economic situation, burgeoning fuel prices and finally the Russia-Ukraine conflict have given a sharp rise to the prices of wheat and its related items.

Ghee and cooking oil are also necessary food items in Pakistan. The nation needs about 4.1 MMT of edible oil each year. Only 11% of the edible oil required for home use was produced in Pakistan in 2021; the other 89% was imported. In Pakistan, the cost of cooking oil has grown by 14.2 percent since the war began, and the cost of vegetable ghee has increased by 15.8 percent in just six weeks. This upward trend is likely to continue since the conflict may cause a significant shortage on the global market for edible oils. [4].

In Pakistan, two types of crop sessions are primarily considered. The first is "Kharif," while the second is "Rabi." Kharif, which is sown between April and June and harvested between October and December Rice, sugarcane, cotton, maize, moong, mash, bajra, and jowar make up most of this season's crop cycle, whereas the Rabi season's sowing takes place from October to December and is harvested from April to May. Wheat, gramme, lentil, tobacco, rapeseed, barley, and mustard make up most of it. Cotton, sugarcane, rice, maize, and wheat are the main crops grown in Pakistan on a big basis. Table 1.1 lists production of important crops [5]

Table 1.1: Major Crops Production in Pakistan (Source: Economic Survey of Pakistan)

Year	Cotton (bales)	Sugarcane (Tonnes)	Rice (Tonnes)	Maize (Tonnes)	Wheat (Tonnes)
2014-15	13,960	62,826	7,003	4,937	25,086
2015-16	9,917	65,482	6,801	5,271	25,633
2016-17	10,671	75,482	6,849	6,134	26,674
2017-18	11,946	83,333	7,450	5,902	25,076
2018-19	9,861	67,174	7,202	6,826	24,349
2019-20	9,148	66,380	7,414	7,883	25,248
2020-21	7,064	81,009	8,419	8,465	27,293

In Agriculture Sector, use of organic and inorganic fertilizers is increasing day by day due to exponential increase in population of the world. After industrial revolution, to fulfill the demands of the growing population, crop production per unit area have been increased along with synthetic inorganic fertilizers. On the flip side of story, the worldwide excessive use of synthetic fertilizers has caused so many health and environmental challenges for humanity on earth.[6].

For extra yield, we use excessive amount of fertilizers which produce dangerous greenhouse gases depleting the protective ozone layer and exposing the human beings to harmful ultraviolet rays [7]. Excess use of Nitrogen fertilizers

cause emission of nitrogen oxides (NO, N_2O, NO_2) which cause severe air pollution in the environment[8]. Methane,CO_2 , hydrogen sulfide and chloro-fluoro hydrocarbons are also responsible for ozone depletion [9]. After CO_2 and CH_4, nitrous oxide has become the 3rd most important green-house gas. Nitrous oxide has 310 more global warming impact than CO2 [7].

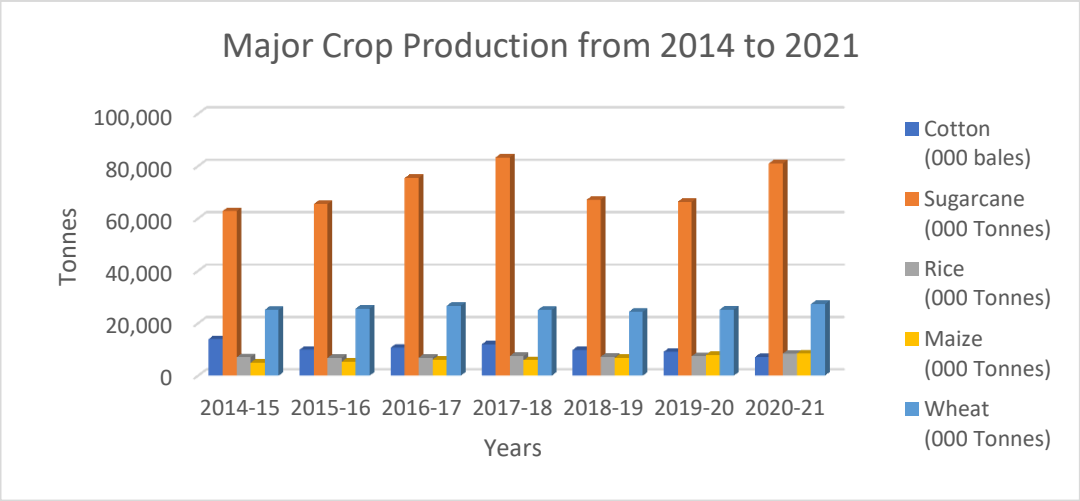

Figure 1.1:Major Crops Production in Pakistan (Source: Economic Survey of Pakistan)

1.2 Pakistan Fertilizer Production and Demands

Pakistan produces around 84% of the fertilizer it needs domestically, with imports making up the remainder. The opening balance for the total area for Rabi 2020–21 was 473 thousand tonnes of urea (Table 2.12). In-country output would total 3,017 thousand tonnes in Rabi 2020–21. In contrast to the 3,490 thousand tonnes of total availability, 3,220 thousand tonnes of urea were off taken during the current Rabi 2020–21, leaving a closing balance of 304 thousand tonnes for the following season. Expected 1,162 thousand tonnes of DAP available for Rabi 2020–21 consists of 347 thousand tonnes of local production, 518 thousand tonnes of imported supply, and 297 thousand tonnes of opening inventory. About 1,059 thousand tonnes of DAP will be taken up during Rabi season, leaving a balance of 101 thousand tonnes for next season[2].

About 3,536 thousand tonnes of urea will be available overall in Kharif 2021, consisting of 304 thousand tonnes of opening balance and 3,232 thousand tonnes of

domestic output (Table 1.2). Around 3,033 thousand tonnes of urea are anticipated to be consumed, showing a closing balance of 503 thousand tonnes. Against an anticipated offtake of 1,012 thousand tonnes, there will be a total of 566 thousand tonnes of DAP available. The private sector will import goods to close the supply and demand gap.[2].

1.3 International Fertilizer Production Capacity and Demands

181.9 million metric tonnes (Mt) of fertilizer were consumed globally in 2014–15, with nitrogen (N), phosphorus (P), and potassium (K) accounting for 102.5 Mt, 45.9 Mt, and 33.5 Mt, respectively. Estimated fertilizer applied to cereal crops was 89.6 Mt, or 49.3% of the total fertilizer applied worldwide. The top three crops for fertilizer use are rice (13.7%), wheat (15.3%), and maize (16.2%). 4.0% of other cereal crops receive fertilizer. Estimated 23.2 Mt of output occurs globally. Around 4% of global applications came from fiber and sugar crops (3.7% and 4.1%, respectively), whereas 2.3% came from roots and tubers. Together, fruits and vegetables made up 15.8% of the global market, with fruits accounting for 7.2% of the total and vegetables for 8.6%.[10].

To get good crop yield minerals and fertilizers are very essential. Fertilizer application since 1950, has been increased day by day drastically. World mineral and fertilizer production have seen continuous increase from 14 to 143 million tons. $N + PO + KO$, nitrogen, phosphate, and potash, are increasing at the rate of 6%/year from 1950-90. International crop production from 1995/97 to 2030 will be increased 57%, according to recent survey of (reference). The crop production rate is greater in developing countries than in developed counties. According to Food and Agricultural Organization, the international use of fertilizer will be increased from 167 to 199 million tons/year by 2030 [11].

Now in the world the people have great worry about the environment. The use of fertilizer is causing environmental problems such as water and soil problems. Nitrate is the primary element of fertilizer, which is the fundamental element to cause water pollution. When Nitrogen dissolves in water, produced nitrate in standing water or other water bodies. When concentration of nitrate in drinking water is greater than 50 mg/L , it can cause many major diseases such as 'blue baby syndrome', gastric cancer, birth defect and heart disease and water surface algae [9]

The world capacity for producing major Fertilizers including Ammonia Phosphoric Acid and Potassium is shown in table (1.2) and figure (1.2) [12].

According to a survey, it might take a few years for agricultural commodity prices to rebound and stock-to-use ratios to return to more favorable levels, assuming ordinary weather conditions and no significant economic or policy changes. At least for the next two to three years, the existing environment is not very favorable for increasing fertilizer consumption.

Table 1.2: World capacity for producing major Fertilizers

Years	Ammonia (N2)	Phosphoric Acid (K2O5)	Potash (K2O)	Total (N2+K2O5+K2O) million tons/year
2016	180,496	57,295	54,638	292,429
2017	184,558	60,224	58,455	303,237
2018	186,974	61,464	61,951	310,389
2019	189,523	62,357	62,055	313,935
2020	187,354	62,612	63,467	313,433
2021	188,908	63,513	63,513	315,934
2022	190,397	63,702	64,553	318,652

According to the baseline scenario, between the base year (the average of the

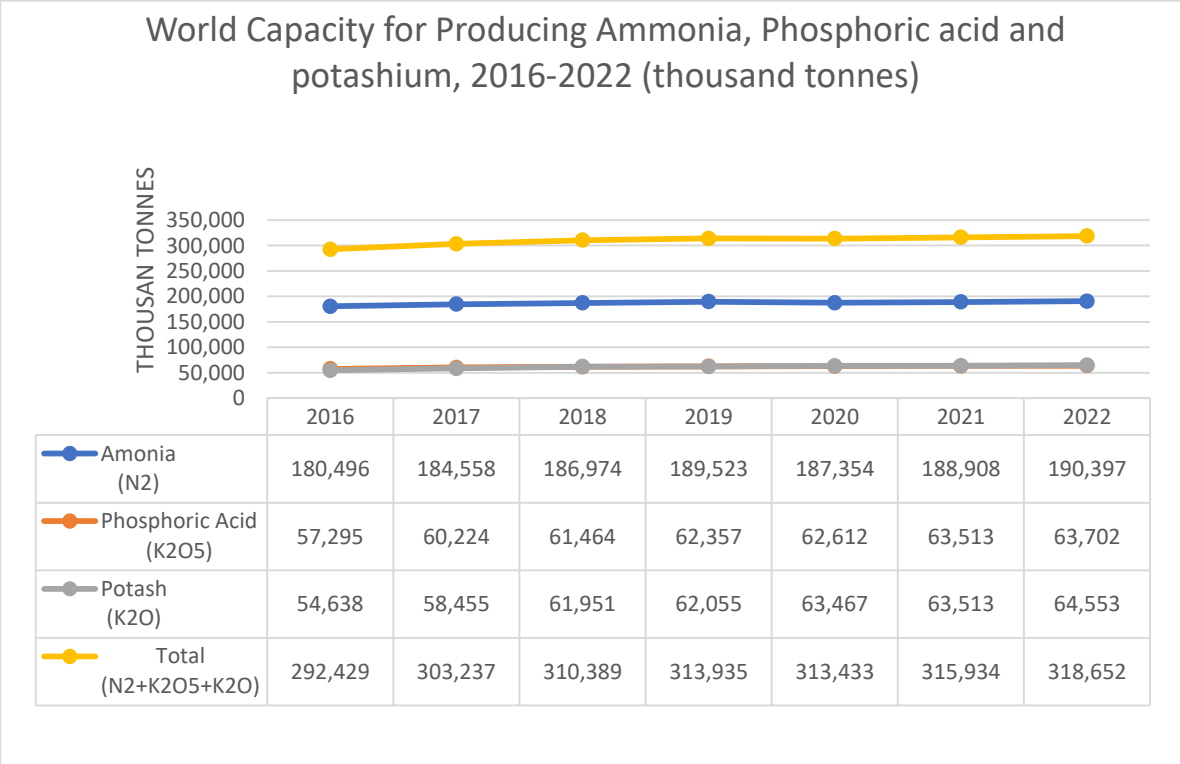

Figure 1.2: World capacity for producing major fertilizers

Years	Ammonia	Phosphoric Acid	Potash	Total
2016	105,148	44,481	35,434	185,063
2017	105,050	45,152	36,349	186,551
2018	105,893	45,902	37,171	188,966
2019	107,424	46,587	37,971	191,981
2020	108,744	47,402	38,711	194,857
2021	110,193	48,264	39,473	197,930
2022	111,591	49,096	40,432	200,919

2012/13 to 2014/15 campaigns) and 2019/20, global consumption would increase on average by 1.7% per year as 200 Mt is predicted to be the total global demand at the end of the projection period.

Table 1.3: World demand for major fertilizers

Figure 1.3:World Demand for major Fertilizers

1.4 Fertilizer Spreading Machines in the World

There are two main categories of fertilizer spreading: one is manual and the other is mechanical. The major techniques are

a. Manual fertilizer is spread by a trained farmer
b. Seed cum fertilizer drill
c. Lawn fertilizer Spreader
d. Tractor mounted centrifugal Spreader
e. Aerial Fertilizer spreader

Altough it offers the greatest degree of control over application rate, spreading

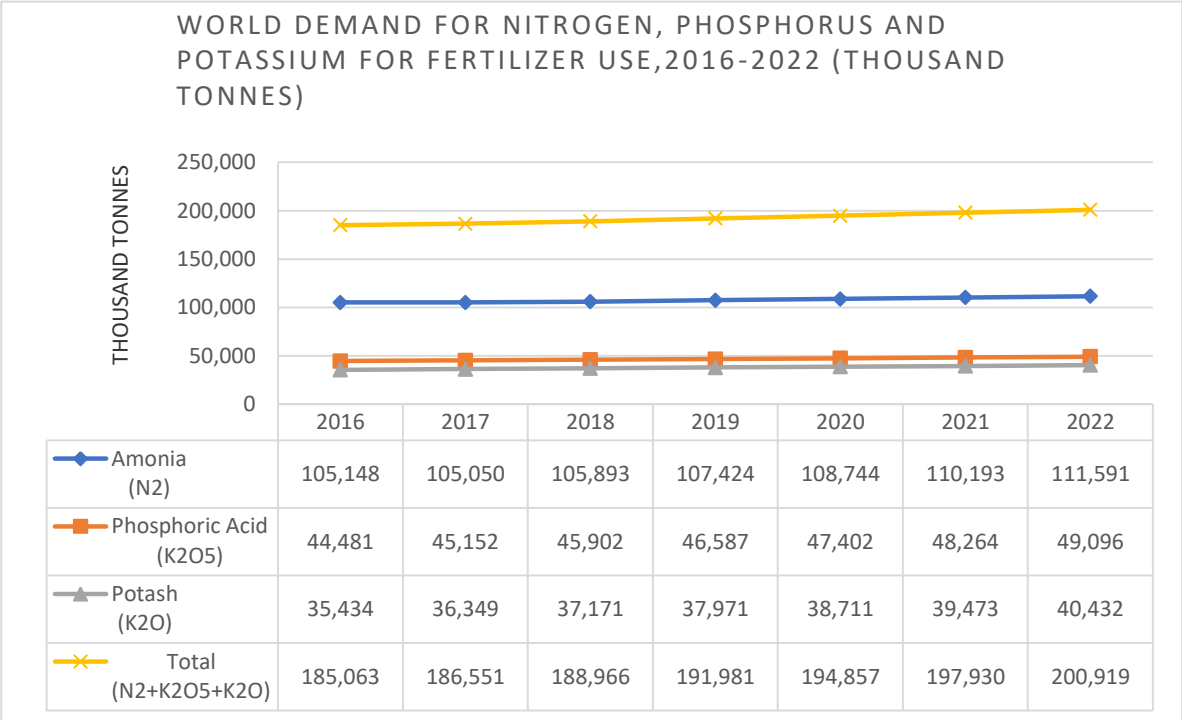

	2016	2017	2018	2019	2020	2021	2022
Amonia (N2)	105,148	105,050	105,893	107,424	108,744	110,193	111,591
Phosphoric Acid (K2O5)	44,481	45,152	45,902	46,587	47,402	48,264	49,096
Potash (K2O)	35,434	36,349	37,171	37,971	38,711	39,473	40,432
Total (N2+K2O5+K2O)	185,063	186,551	188,966	191,981	194,857	197,930	200,919

fertilizer from the ground is the most effective method. Additionally, manual fertilizer spreaders may only fertilizer up to 8 to 10 acres per individual. Some of the area in Pakistan are fertilized by using ground machines, like as drill machine and planter which also have limitations, Manual methods can be used only at earlier sowing stage of the crop and cannot be used at when the crop has grown and in wet soil.

In Pakistan, small-scale farmers use manual agricultural methods for pesticide applications and only a few landowners are using aerial spraying techniques. This is used only when the land is wet, water is standing, and the access of ground is difficult. Granular aerial fertilizer spray is the only solution for Rice, sugarcane, and maize crops for uniform and perfect amount of fertilizer applications. Aerial fertilizer spreader is flexible and time saving. It saves high amount of fertilizer, covers more spreading width, and apply uniform spreading. The most common type of aerial fertilizer spreader is a drone-borne aerial fertilizer spreader as

Figure 1.4:Multi Rotor Drone-Borne Aerial Fertilizer Spreader

you can see in figure (1.4).

1.5 Significance of Drone Technology in Agriculture

A drone is an aircraft without a human pilot on board that is piloted either remotely by a pilot on the ground or autonomously by onboard computers. Other words are also often used, including low-altitude remote sensing, unmanned aerial vehicle (UAV), unmanned aerial system (UAS), and remotely piloted aircraft. [13], [14]

Drones' ability to move quickly and maneuver to desired locations make it one of the most important uses of this technology in agriculture. Drones with this capability can spray pesticides and fertilizers to nourish crops and supply them the nutrition where and when it is required. Crops can be healthy and prosper with the help of such supplements. The drone pilots are free to watch as the drone sprays nutrients to ward off pests, worms, and insects and lengthen crop life.

Drones' powerful powers aid in the rudimentary process of assessing the health of the soil. In essence, UAVs gather and analyze data from monitoring that can aid in assessing, regulating, and maintaining the character and health of the soil. Additionally, drone technology can give soil the vital nutrients it needs to be healthier and more productive. Drones can perform this analysis of soil health because to their capabilities of 3D mapping and data processing. Overall, drones and their applications have made the laborious procedure associated with agricultural fertilization easier. They greatly assist farmers with a variety of duties and operations because of their resourcefulness and enterprising spirit.

1.6 Different Types of Drones

Drones can be utilized in non-military settings. They can be grouped according to a variety of traits. Size, cargo, flight range, and endurance are common factors, as well as the aerodynamic flight concept. These elements work together. A larger drone, for instance, has a greater payload capacity and a greater range and flight time.

Based on the principles of aerodynamic flight, drones can be classified as either fixed-wing or multi-rotor. [13]. Each of them flies using a different set of principles and has advantages and downsides. A multi-rotor drone is propelled by rotor motion. The propellers are in a plane that is perpendicular to the earth's surface. To increase flying stability, it has a system that applies the opposite force to combat the wind. When a multi-rotor drone can do vertical take-off and landing, it gains popularity because of its capacity to function in situations where there is a lack of space (VTOL). However, a multi-rotor has a poor efficiency. On the other hand, a fixed-wing drone requires more space for takeoff and landing and drifts more in windy conditions. However, it frequently has better endurance, allowing one to travel farther with only one sensor and the same flying altitude. Both types of drone are shown in figure (1.5) [15], [16]

Given that it only has one rotor, a helicopter might be thought of as a specific case of a multi-rotor drone. Additionally, hybrid drones are now being developed. These drones fly like fixed-wing drones but have a VTOL feature like a multi-rotor drone. They therefore have the benefits of the two categories. When choosing a drone, price is a key deciding element, and a multi-rotor is comparably less expensive. The decision, though, is based on the specifications of the project.

Figure 1.5:(a) Fixed Wing Drone (b) Multi Rotor Drone

1.7 Goal and Scope

The main aim of this research is design and development of Aerial Fertilizer Spreader, which encompasses maximum coverage, maximum spreading width and compatible with all unmanned vehicle whose weight carrying capacity is 10-12 kg. Deposition of granular fertilizer from impeller which are attached under the UAV. In an ideal case, uniform fertilizer distribution with maximum coverage is the main target. This is not achieved in real case. Simulation on computer save time and money. It helps to analyze various factors and arrive at the uniform combination of adjustable variables[17].

Following aims have been established.

1. Create a model or simulation of the particle trajectories and investigate how physical characteristics affect the trajectories and spread.
2. Modify the trajectory model to fit a particular category of unmanned aerial spreading systems for fertilizer.

3. During routine trials, run experiments on the spreader system to determine the deposition patterns.
4. Run tests with the spreader system to determine flow rates and how meter adjustments affect flow rates.
5. Thesies orginaze in such a way.

Chapter 2 Past work and Theory: in this chapter we discuss about particle motion in the spreader and particle motion in thorough air.

Chapter 3 devoted to Design and fabrication of Aerial Fertilizer spreader/ Mathematical Equation to decide optimized angles, impeller length, motion inside impeller, Motion of projectile

Chapter 4 Experimental Study of Fertilizer Spreader

Chapter 5 Simulation study, effect of particle's physical properties, effect of release velocity and height of particle.

Chapter 6 Conclusion and future work

Chapter 7 Reference

Chapter 2 Literature Review and Previous Work

2.1 Introduction

Food security has become a burning issue in all over the world due to disastrous climate change. According to United Nations Framework for Climate Change (UNFCC) Pakistan is ranked at sixth position in the list of ten most vulnerable countries. Due to havocs of climate change, Pakistan is facing severe food security problem since last two decades. The import bill of food related items is increasing and putting some extra burden on economy of the country. The primary goal of national food security is the spatial information on crop growth status and yield. For much agricultural research, such as evaluations of production predictions, phenology inversions, and spatiotemporal cropland patterns, crop maps are crucial.

The use of UAVs is increasing day by day. These machines provide real time data for application of fertilizers and water requirements in the fields. Moreover, these machines are helping to predict the future requirements of rain and soil treatment also. The UAVs are being used in agronomy, application of irrigation systems, assessment of health of crops, disease prevention spray and real time monitoring of crops. The UAVs can be classified into various ways. Three main categories are: classification based on their application, based on their carrying capacity and on the basis of their wing's formation. Fertilizer's particle motion is another important area while using UAVs in the fields. Particle motion through the spreader and particle motion through the air are two key areas used for further calculation of requirement of field, carrying capacity of UAVs, and amount of fertilizer to be spread in all directions.

2.2 Agronomy Applications of UAVs

Before delving into the specifics, it's critical to comprehend how UAVs launch and carry out their various tasks. We must understand the principles of a standard UAV's development and structure. Different UAVs are constructed from a variety of lightweight materials to reduce their weight and increase their rate of flight mobility. These can also be equipped with other necessary components, such as

cameras, GPS units, GPS-guided rockets, navigation systems, and sensors.[18]. UAVs come in a variety of types depending on their price, capacity, capacities, forms, and functions. The current models have manual launch capabilities and can be operated with remote controls or from specialized ground cockpits. The streamlined UAVs are created for industrial uses. Given that they are lightweight but challenging to handle and come in a variety of shapes and sizes, the vehicle is reasonable and appropriate for children. One of the most important components of every UAV is the watertight engine structure. In addition, flight engine controllers, motors, transmitters, receivers, propellers, and batteries are other energy sources.[19].

Agriculture is a crucial subject of study that can benefit from the use of contemporary technology. Humans are entirely dependent on agricultural produce for their food. The market demands cannot be addressed by the conventional ways. Population growth is linearly rising over time. However, due to low agricultural production and cultivation, the issue of feeding a growing population globally is becoming more complicated. The effects of climate change disasters, water scarcity and waste, the blending of chemicals with the harvest, and greenhouse gas emissions have worsened this issue. With the introduction of smart farming, new digital technologies will help to resolve these problems and usher in a new era. [20]**.** Utilizing UAV technology can help enhance agricultural operations. Large gains can be attained by using UAVs and innovative cultivation techniques, including quick and accurate soil analysis, quick and uniform fertilizer application, monitoring of crops and their demands, and precise use of irrigation systems like tube well. [21].

2.3 Use of UAVs in Irrigation Systems

The application of UAVs to provide 3-D mapping for preliminary soil analysis, which is helpful for future decision-making, is at its beginning stage. The UAV-based system offers information that may be used for irrigation, nitrogen level monitoring, and the administration of the correct amounts of fertilizer to crops in order to safeguard soil fertilization. The soil will receive the correct nutrients and support healthy growth through this technique. [22]. It is well known that a precise irrigation management system depends on accurate field estimations of soil moisture content (SMC). Due to their high cost and limited scope of monitoring, the current ground-based methods for measuring SMC are limited and unfavorable. Unmanned

aerial vehicle (UAV) development offers a practical method for measuring SMC on a big scale.[23].

2.4 Deployment of UAVs in Health Assessment of Crops

There are different health issues regarding crops, its soil, its fertility, its seeds and its yield. The major issue is to spots bacterial and fungal infections. The crop scanning and its assessment is essential for providing an immediate treatment to the field to save its yield. In past, the conventional methods were used as the use of naked eye or mini lab methods which were usually time taking and less accurate methods. Hence the conventional methods of assessment are no more useful for modern diseases and their treatment. The use of visible, near infrared and Agrocam light methods have become obsolete. The deployment of UAVs is the best technique and assessment method through which the scanning of crops can be done very easily in order to identify its diseases, provision of its treatment and other agronomy measures for high production rates.[24].

2.5 Use of UAVs in Plant Prevention Spray

The technique that uses ultrasonic and lasers to measure distance can be used to detect light and set the LIDAR range, which allows UAVs to adjust height in relation to topography and landscape. Additionally, all UAVs are outfitted with this LIDAR technology for scanning the ground so that spraying operations can be carried out with the precise amount of liquid and at the appropriate distance from the ground. This method will limit the amount of chemicals that seep into the soil, boost its effectiveness, lessen water contamination, and cut down on the time needed to complete the task. According to estimates, using UAVs to spray chemicals is five times faster than using manual labor or more conventional machinery.[20].

2.6 UAV in Monitoring Crop

With the passage of time, different areas are being monitored in different ways to monitor all types of crops, weather conditions and their needs of fertilizers. Furthermore, the traditional monitoring system of crops have become outdated, obsolete, and not working properly. Satellite photography is also losing its importance as low quality images can misguide the decision-making process. Hence,

to cover all these drawbacks UAVs are being introduced in agricultural fields. These UAVs are very important for monitoring of crops, for collection of high-quality images ,for taking of right decision at right and for timely spray of fertilizers in the fields. [25].

2.7 Classification of UAVs

There are three types of UAVs that can be classified based on the area of applications, their carrying capacity and their wings.

2.8 Classification of UAVs based on their Applications

Depending on the application, we use multispectral, hyperspectral, or thermal sensors that can identify the real irrigation, chemical, and fertilizer demands of a field. Additionally, the UAVs can begin the calculation of the vegetation index. This indicator details the physical condition, total energy used, and temperature emitted by the crops in addition to their practical concentration.[26]. First RS usage for precise measurements of cropland have been documented in 1930s and practically applied since 1950s Since then, satellites have scanned the planet and its crops to monitor temperature and spectrum reflectance characteristics that are also important for farmers. The crop's health can be determined by the temperature. Currently, one can learn how much carbon is absorbed by trees, how much water is utilized for certain fields, and even forecast how much water will be required by a specific crop or a specific product by turning satellite data into vapor-transpiration images. Most farmers around the world are unable to use that information properly. One of the most well-known fixed-wing drones, Lancaster carries the most aerial sensors and provides accurate aerial data. diverse areas that are small, restricted, and irregular. Precision imaging and operation are better suited to multi-rotor drones. The Guardian-Z10 drones can quickly replace manual labor in the fields by combining low-cost equipment with highly effective pesticide spraying. It guarantees minimal pesticide penetration and improved spread accuracy to minimize pesticide residue and boost output. With proximity detectors, it can fly by itself across uneven terrain. The DJI Agras MG-1S, a hexacopter and octocopter with a similar modular design, can cover up to 6000 square meters in 10 minutes while carrying up to 10 kg of fertilizers, insecticides, and herbicides, which is 60 times faster than human spraying. Due to radar-based detection, the MG-1S automatically adjusts its spray to

the flying speed and height over the crops. The categorization of civilian drones' states that there are seven UAV classes based on size, flight time, and capabilities (Fig. 2.1). The biggest platform is HALE UAS in comparison to other satellites-based systems. It provides significant cost savings solutions along with multiple parameters and diversified options [27]

Table 2.1:Popular universal Fixed-Wind and multi-rotor Drones for Agricultur

Sr. No	**UAV classification**
a.	Nano Air Vehicle, Prox Dynamix Black Hornet [28]
b.	Micro Air Vehicle, AeroVironment Microbat [29]
c.	Vertical Take-Off and Landing, Aeryon SkyRanger R60 [30]
d.	Low Altitude, Short Endurance, AeroVironment Puma AE [31]
e.	Medium Altitude, Long Endurance, NASA's Ikhana Predator B [32]
f.	Close with longer endurance, Low Altitude, Long-Endurance - Boeing Insitu ScanEagle [33]
g.	High Altitude, Long Endurance, Airbus Zephyr T[34]

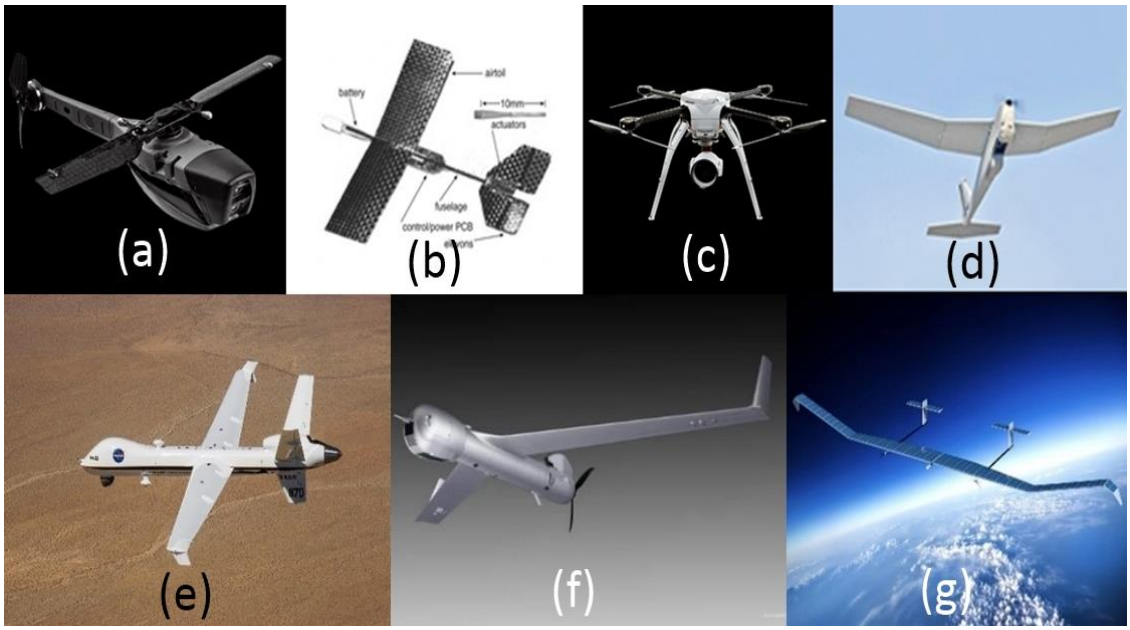

2.9 UAVs Classification based upon their Carrying Capacity

As the population grows, the risks of food insecurity rise daily, making the ceaseless improvement in agriculture both disgusting and necessary for humanity. Agricultural advances have socioeconomic advantages; they increase agricultural yields, create job possibilities, and lessen the employment gap between rural and urban areas. [35]. Precision agriculture is a cutting-edge method of managing agriculture that uses modern technology to monitor crop performance and implement strategies to increase agricultural yields. [36]. It is revolutions in agricultural fields[37]. It is "an agricultural system where management practices are carried out at the proper location, with the proper level of intensity, and at the proper time."[38]. Precision agriculture has recently experienced a boom thanks to advancements in unmanned aerial vehicles (UAV), which combine with image data analytics to offer

Figure 2.1:Popular universal Fixed-Wind and multi-rotor Drones for Agriculture

answers to problems including climate change, a lack of potential arable lands, and the demand for freshwater. [39].According to [38] Precision agriculture has seen a "game changer" thanks to UAV technology. UAVs can be utilized in precision agriculture in a variety of ways, such as crop monitoring, crop height estimation, pesticide application, soil analysis, etc. Similar to this, the UAV's imagery is being employed for early crop disease identification. [40]. Therefore, precision agriculture may be done effectively using UAVs. UAVs can significantly lower the cost of using pesticides, fertilizers, and water. UAVs can be categorized according on how much fertilizer they can carry at once. Table 2.2 UAVs classification based upon storage capacity.

Table 2.2: UAVs classification based upon storage capacity.

Sr No	UAV classification
a.	5-liter S1000 Drone
b.	DJI, 10 liters
c.	DJI, 16 liters
d.	DJI, 30 liters

2.10 Classification of UAVs based on Wings.

It is also possible to categorize UAVs according to the precise sort of wings they have. A typical type of unmanned aerial vehicle (UAV) with fixed wings (Figure *2.3)[41] has immovable* arms that can be operated manually or automatically.

Figure 2.2:Fixed Wing UAV

Figure 2.4:Hybrid UAV

Hybrid vtol is another traditional wing-based UAV design (Figure 2.4)[42]. Additionally, it is also referred as a fixed-wing jet, or a hybrid unmanned aerial vehicle VTOL aircraft [22]. A multi-rotor design that inseparably links four or more propellers allows a hybrid UAV or VTOL to function in practically any scenario.

For field mapping and livestock management, fixed-wing UAVs are already widely used. The Fixed-wing UAV is more dependable and less expensive than other UAV models due to its simple design and control principles. However, hybrid VTOL UAVs are incredibly influential for their effective combat strategies, which might be useful for agricultural consideration.

There is a third type of UAVs called rotatory wing UAVs. These are composed of two or three revolving mechanism blades that are structured into a rotor-like structure and revolve around a fixed pole. Rotor blade operation is comparable to that of a fixed wing. The rotor's settings do, however, have advantages and disadvantages. There are two additional categories for rotary-wing UAVs: single and multi-rotors. Multi-rotor UAVs are the most trustworthy wing-based UAVs. Multi-rotor platforms are swift and nimble and are capable of successfully completing difficult maneuvers. The previous ten years have seen the most significant technological advance. There are equally numerous models of Multi-rotor UAVs i.e.,

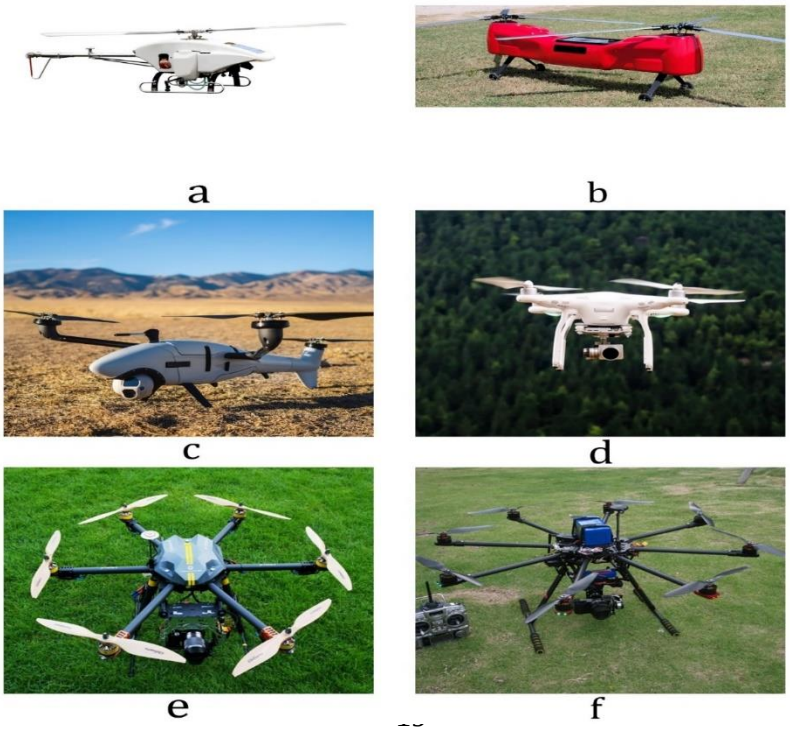

Figure 2.5:Different types of drones

helicopter figure(2.5a), Dual Motor (figure 2.5b), Tricopter (figure 2.5c), Quadcopter (figure 2.5d), Hexacopter (figure 2.5e) and Octocopter (figure 2.5f).

2.11 Fertilizer Particle Motion

The application of mineral fertilizers is a crucial procedure that guarantees a consistent crop production over the field area along with its good yield. Currently, most mineral fertilizers are spread on the ground utilizing machines that have centrifugal spreaders. Utilizing centrifugal spreading tools, whose rotation axes are inclined at an angle to the horizontal plane, is one way to improve uniform distribution of fertilizers on the field surface.

From the spreader device where they are metered until they hit the ground, particle motion can be separated into

(i) Particle motion within the spreader device

(ii) Particle motion through the air and. Physical properties of the particle can have different and even opposite effects for both motions [43].

2.12 Particle Motion through Spreader

The centrifugal fertilizer spreader is a highly efficient device being used by farmers to save their time and increase their yield throughout the world. Typically, they consist of spinning discs including two anticlockwise discs. These machines are popular due to their low cost, simple upkeep, and a big working breadth up to 36 meters (more than 15 times the machine width). These spreaders have predominated in use thus far for evenly applying fertilizer to the field.

Leaching to ground and surface water is minimized when fertilizer is provided in accordance with site-specific needs, but at the same time, a considerable amount of fertilizer is necessary for required yield. Moreover, it has been reported that under-dosage results in yield inefficiencies [44], [45]. There is a requirement for site-specific application to a system of automatic controls that can change spreading mass flow rates according to the needs.

Spreader use map and different techniques such as global positioning system (GPS) to locate different requirements in the field. Given the parameters of the fertilizer, a model simulating the spreader action is required to construct such a control system. A spinning disc fertilizer spreader simulation model was described by [46].This mechanistic model tracks the movement of fertilizer particles as they

fall onto a rotating disc spreader, through the flow of the spreader, as they are launched into the air, and to their landing place on the ground.

2.13 Particle Motion through Air

Particle motion through the air is independent of the spreader. Only the initial velocity and direction of the particle as it comes out of the spreader is determined by the spreader.

The forces acting on a particle moving through air Include, buoyancy force, gravitational force, inertial force, and frictional force. The buoyancy force can be neglected if the density of air (ρ_a) is much smaller than the density of the particle (ρ_p). A set of differential equations, using the balance of the remaining three forces, describe motion of the particle completely. Real particle trajectories are found to deviate only slightly from the theoretical particle trajectories[43]. The sight variation may be caused by the eventual tumbling or rotating of the particle. Reints and Yoerger (1967) [47] derived the equations 2-1 and 2-2to describe two-dimensional motion of the particle in air (Fig. 2.5)

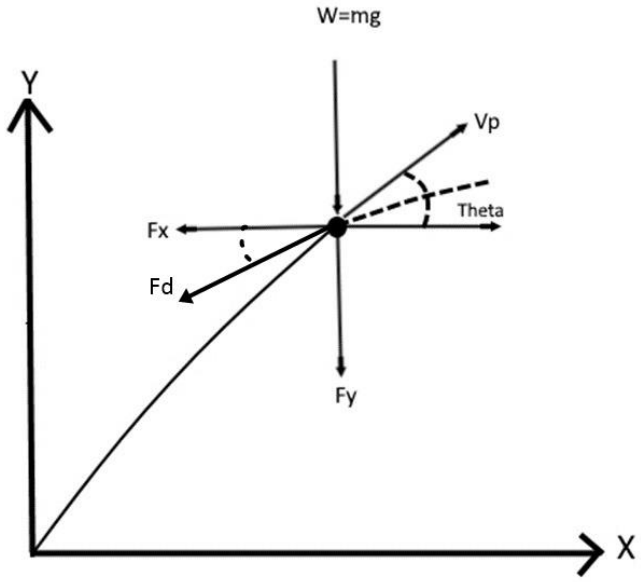

Figure 2.6:Two-dimensional projectile motion of a particle

According to newtons 2nd law sum of forces in one direction is equal to product of mass and acceleration in that direction:

$$m_p \frac{d^2x}{dt^2} = -F_{dx} cos\theta \tag{2.1}$$

$$m_p \frac{d^2y}{dt^2} = -m_p g - F_{dy} cos\theta \tag{2.2}$$

The drag force, F_d is given by:

$$F_d = \frac{1}{2} C_d \rho_a A_a V_p^2 \tag{2.3}$$

where V_p, is the velocity of the particle, m_p represents mass of the particle. g is the acceleration due to gravity, V_p represents the drag coefficient, ρ_a, is the air density, and A_p, represents area of particle projected on a plane normal to the direction of Coefficient of drag, C_d, is a non-dimensional number, value of which depends upon the particle properties and flow condition. Many empirical relations have been suggested by researchers which relate C_d to another non-dimensional number known as Reynolds number,R_e . The Reynolds number is given by:

$$R_e = \frac{\rho_a V_a d_p}{\mu_a} \tag{2.4}$$

Where, d_p, is the diameter of the particle, and μ_a is the coefficient of dynamic viscosity of air. is a material property and varies with the air temperature. For dynamic viscosity of air, the following relation can be used [48]:

$$\mu_a = \frac{0.0076342}{T_a + 296.16} \left(\frac{T_a}{296.16} \right)^{1.5} \tag{2.5}$$

where, $T_a$is the ambient air temperature which are taken in kelvin. Figure 2-4 shows how C_d changes with R_e [49].

At low Reynolds number ($R_e \cong 0.1$)., the flow is known as Stokes flow and under these conditions, the coefficient of drag, *Cd* is given as,$\frac{24}{R_e}$. At high Reynolds number ($R_e \approx 10^3$) the due of C_d becomes approximately constant at about 0.4. When the Reynolds number is within the intermediate range, which is the range of practical interest, the coefficient of drag, C_d varies with Reynolds number in a complicated manner [50],[47] fitted an exponential curve and obtained the following equation:

$$C_d = e^{(0.1960\, log\, Re - 1.885)^{2.337} - 0.9560} \tag{2.6}$$

They solved differential equations (2.1) and (2.2) numerically, using the C_d from equation (2.6). The trajectories for a variety of materials and several initial conditions were determined. The simulated horizontal distances were compared with the experimental observations. It was found that almost all calculated and measured

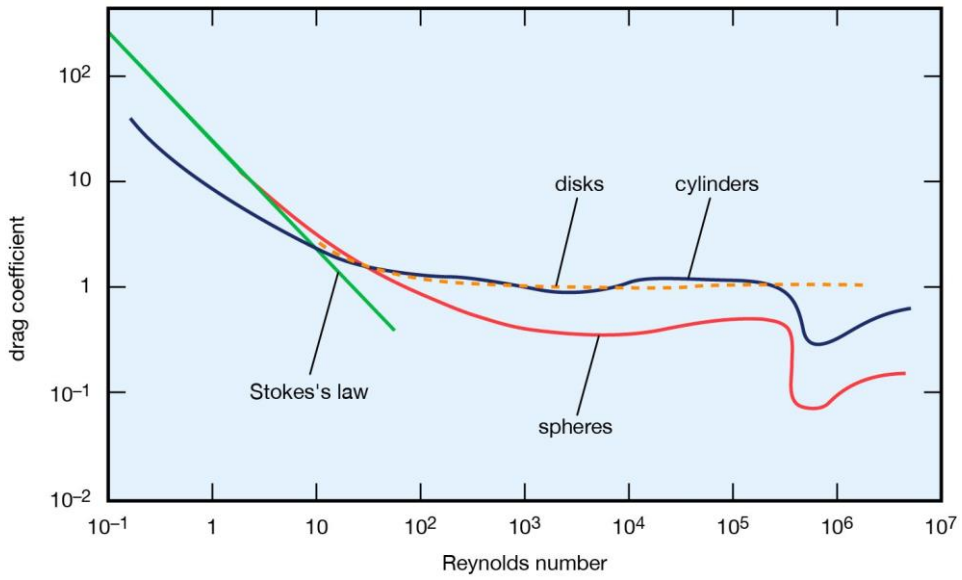

Figure 2.3: Variation of Coefficient of Drag with Reynolds Number

trajectories were within 10% of each other.

The velocity of a particle moving in a fluid change continuously, until it attains terminal velocity. The Reynolds number, and thus the coefficient of drag depends on the velocity of the particle. Therefore, to calculate the trajectory of a particle moving in a fluid, the instantaneous coefficient of drag must be known. Since no mathematical relationship is available, which would make it possible to calculate it analytically, either an indirect method or an empirical formula must be derived. Many researchers-have formulated empirical relations by fitting an exponential curve to the experimental data points relating C_d to the Reynolds number.

Khan and Richard [51] derived the following relation, after using a nonlinear regression on 300 data points:

$$C_d = (2.25Re^{-0.31} + 0.36Re^{0.06})^{3.45} \tag{2.7}$$

Proposed [52] by Flemmer and Banks Re < 8.6×10^4:

$$C_d = \frac{24}{Re}10^E \tag{2.8}$$

where,

$$E = 0.261Re^{0.369} - 0.105\,Re^{0.431}\frac{0.124}{1 + (log_{10}Re)^2}$$

Turton and Levenspiel [53] presented the following relation:

$$C_d = \frac{24}{R_e}(1 + 0.173Re^{0.657}) + \frac{0.413}{1 + 16300Re^{-1.09}} \tag{2.9}$$

Haider and Levenspiel [54] suggested the following equation:

$$C_d = \frac{24}{R_e}(1 + 0.1806Re^{0.6459}) + \frac{0.4251}{1 + \frac{6880.95}{Re}} \tag{2.10}$$

The goodness of fit, as measured by mot mean square (RMS) deviation of these empirical relations [55] are presented in Table 2.3.

Table 2-3:RMS deviation of range of Reynolds number

Equations	**Range**	**RMS Deviation**
2.7	$Re < 3 \times 10^5$	0.041
2.8	$Re < 8.6 \times 10^4$	0.066
2.9	$Re < 2.6 \times 10^5$	0.025
2.10	$Re < 2.6 \times 10^5$	0.024

For non-spherical particles a non-dimensional number, to account for part ideal shape, *(φ)* is first defined:

$$Sphericity = (\varphi) = \frac{A_s}{A_S}$$

where A_s is the surface of a sphere having the same volume as non-spherical particle and A_S is the actual surface area of the particle. Sphericity gives a measure of how close a particle shape is to the spherical shape. It can be readily calculated that a cube has 0.806 Sphericity and a tetrahedron has 0.607 Sphericity. Haider and Levenspiel [54] suggested the following relation to calculate the coefficient of drag of non-spherical particles:

$$C_d = \frac{24}{Re}(1 + (8.1716e^{-4.0655\varphi}) + \frac{78.89Re(e^{-5.0748\varphi})}{Re + 5.378e^{6.2122\varphi}} \quad (2.11)$$

The accuracy of equation (2-11) depends upon the Sphericity of the particles. It is reported to vary from 4% to 22% depending upon the particle shape and Sphericity [54]. The range of Reynolds number is given as, $Re < 2.5\,x\,10^4$.

Chapter 3 Model Development and Mathematical Review

3.1 Introduction

Designing is an iterative process, and it depends upon the requirement of the user. In mechanical design various parameters and criteria have been included, some of them are safety, function, weight, size, reliability, manufacturability, wear and tear, liability, and material selection. Recent design is a complex process that combines various factor such as Technical and engineering Familiarity, creativity, proper management, interpersonal relationship, best supply chain and optimum method of manufacturing. Design and material selection is based on our requirements. For designing of aerial fertilizer spreader, solid works is used, and for static analysis Ansys is preferred. In next phase mathematical model is developed to find the required parameter such as angle of projection, length of impeller, and optimize velocity. MATLAB software is used to determine the design parameter of aerial fertilizer spreader. To study the particle trajectory model, we consider a spreader ejecting a particle of mass M_p, diameter D_p, density ρ_p height of H. The initial velocity of particle is V_{p0}. To estimate the final location of particle on ground first we must analyze the initial velocity, direction, and trajectory of particle. There are four forces acting on particle once it is out of spreader i.e., buoyancy force, gravitational force, inertial force and drag force

Due to low air density than particle, buoyancy force can be neglected[43] so we are left with remaining two forces which will describe the motion of particle in the $x\ and\ y$ direction and components of drag force F in x and y direction. We describe our problem into three different phases, (i) Designing of Aerial fertilizer spreader, (ii) motion inside impeller, (iii) motion into the air.

3.2 Design of UAVs

Nowadays hexacopters and octocopters are gaining more popularity as they have a number of advantages over quadcopters [56], [57]. Hexacopters, for instance, have more fault tolerance than quadcopters and can carry more weight. They also

have longer flown times. Additionally, using multiple motors reduce the length of the blades, resulting in fewer structural and dynamical issues. They can adjust the distance from the ground and spray in real time for even and smooth coverage, boosting the field's overall effectiveness [58]. In essence, a hexacopter is a 6-rotor helicopter. Its thrust, or upward force, is evenly distributed across its six rotors, and additional movements can be controlled by changing the motors' speed. The six clockwise and counterclockwise rotors on a hexacopter combine to produce the upward propulsion, eliminating the need to oppose aerodynamic torque forces. Figure 3.1 shows a hexacopter with basic components. It halves the thrust required for flying by 1/6 for each rotor, allowing for the use of less potent motors that can aid with cost-cutting without sacrificing overall efficiency.A hexacopter consists of the following parts Motor, Propeller, Flight Controller Transmitter and Receiver and Battery.

3.3 Design of Fertilizer Spreader

Customize design is an iterative process. A fertilizer spreader as shown in figure in (3-2) consists of a hopper, motor, and centrifugal impeller for spreading of fertilizer. The material used for this customize fertilizer spreader are carbon fiber, Stainless steel and 3D printed part. The flow rate adjustment is done with up and movement of impeller which shown in figure (3-3) which is attached at the bottom of hopper. Its rotating speed is continuously adjustable, fertilizer drop in impeller due gravity and then move out of impeller due to centrifugal force. Dimensions of fertilizer spreader are given in figure (3-4) and Overall specification is mentioned in table (3.1).

Table 3.1 Specifications of Aerial Spreader

UAVs Components	Specifications
No of wings	6
Motors	6
Take-off weight	24Kg
Flying speed	0-8 m/s
Flying height	0-30 meters
Fertilizer tank capacity	10 kg
Number of Impeller	2
Spreading Pattern	Centrifugal Spreader

Figure 3.1 Hexacopters

UAV Size (W*L*H)	2.0 ×1.3×0.45 m
Spray span	>2-20m
Spray efficiency per hour	≥1.5 hectares
Flight time	10-15mints

To store granular fertilizers, hoppers are used which are large barrel-like containers which shown in silver color in figure 1.2. On the drone, there are two hoppers on each side to maintain symmetry and balance. The storage capacity of hoppers depends upon payload capacity of the drone. The mass of granular fertilizers sprayed in one flight depends upon the size of hopper. There must be balance between the hopper size and load the drone can carry. This is another advantage of granular fertilizers because unlike liquids they are in concentrated form of matter.

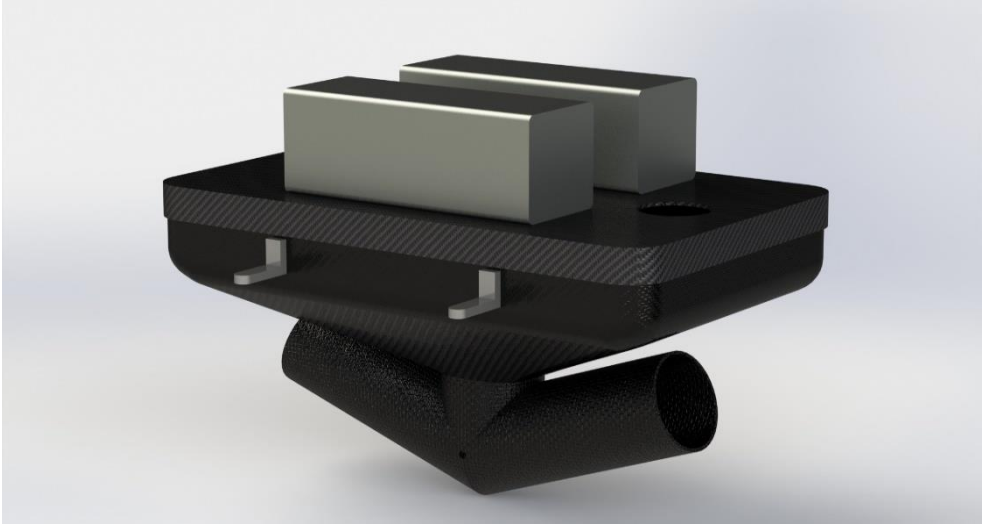

Figure 3.2 3D model of a Fertilizer Spreader

The metering device is an auger which is driven by motor and installed at the bottom of hopper. The speed of auger is constant and fertilizer flow is controlled by sliding plate.

To disperse fertilizers there are two openings on each side which allow same amount of fertilizer to flow through each side. The quantity of dispersion is controlled by deflector plates.

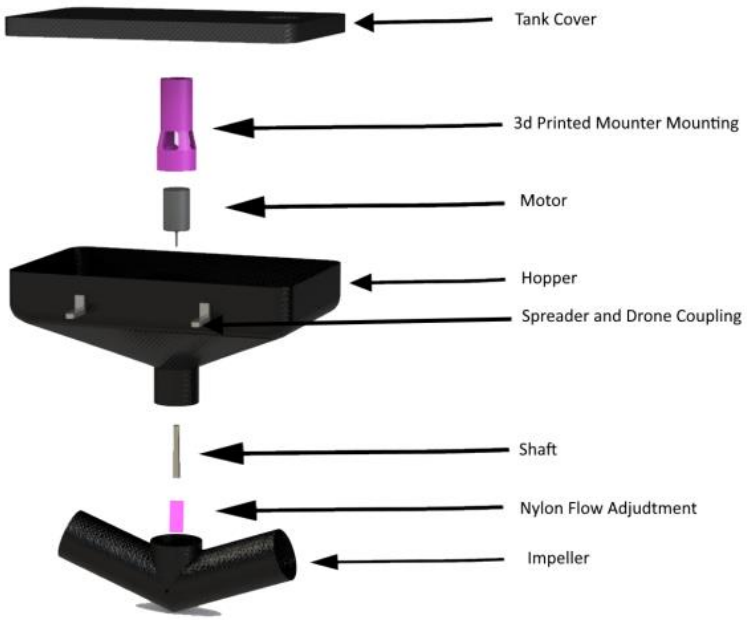

Figure 3.3 Exploded view of fertilizer spreader

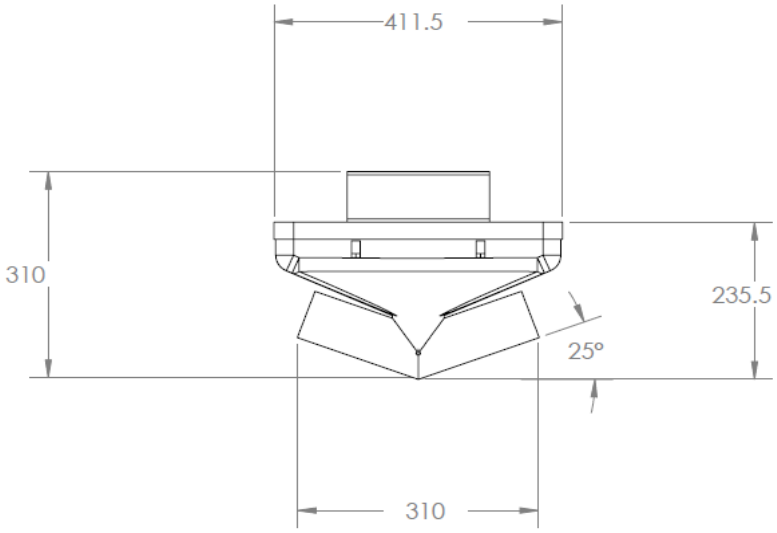

Figure 3.4:Dimension of fertilizer spreader

Table 3-2 Specifications of Fertilizer Spreader

Sr no.	Project	Attribute
1	Overall size	310mm X 411.5mm X 235.5mm
2	Hopper	Carbon fiber
3	Flow rate adjustment	3D printed
4	Impeller	Carbon fiber

3.4 Drone and Spreader Assembly

Drone and spreader assembly shown in figure 3.5 and overall dimensions are shown in figure 3.6

Figure 3.5: Drone and fertilizer spreader

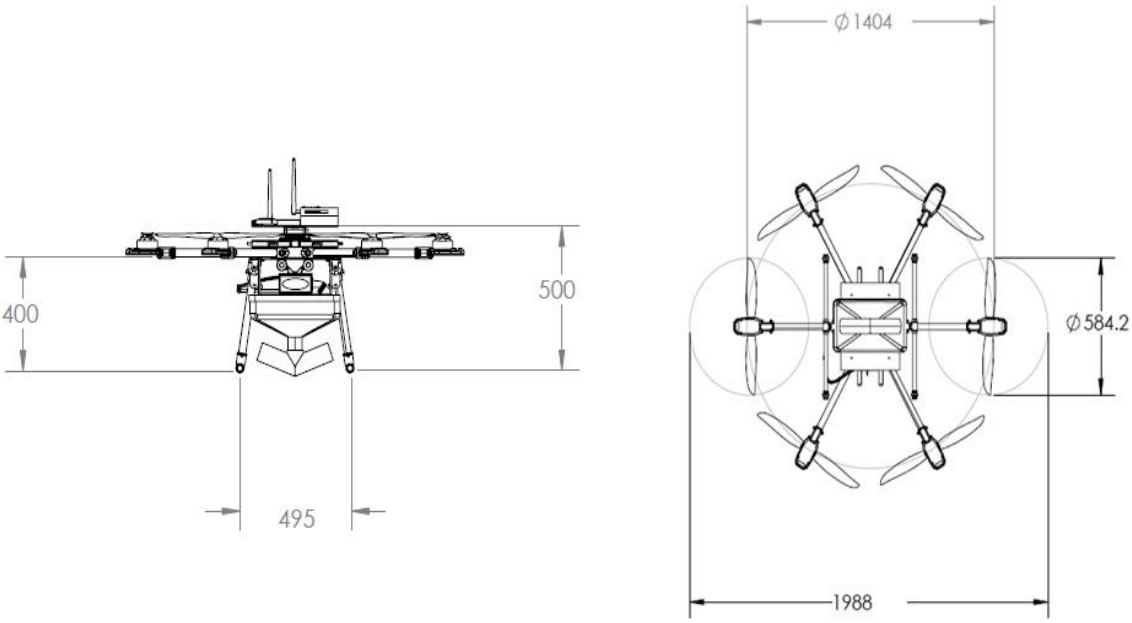

Figure 3.6:Dimensions of Drone and Fertilizer Assembly

3.5 Kinematic Analysis of Fertilizer Particle Motion within Spreader

When fertilizer seed fall under the action of gravity in non-inertial reference system they will be ejected from impeller under the action of centrifugal force. When the fertilizer particles move in impeller, they will face frictional forces from the

impeller, thrust from pipe and Coriolis force. Fertilizer particle ejected from impeller and move inside pipe. The kinematic analysis of the fertilizer particle following impact to their initial velocity and angle of impeller [59].

we can write the position, velocity, and acceleration of point P with respect to point O measured in the inertial frame as follows:

$$Position = r\hat{e}_2 \tag{3.1}$$

$$Velocity = \dot{r}e_2 - r\omega \sin\theta\, e_3 \tag{3.2}$$

$$Acceleartion = -\mathrm{r}\omega^2 \sin\theta \cos\theta\, e_1 + (\ddot{\mathrm{r}} - \mathrm{r}\omega^2 \sin\theta^2)\hat{e}_2 - 2\dot{r}\omega \sin\theta\, e_3 \tag{3.3}$$

$\ddot{r}$ = *Linear Acceleration in the radial direction*

To implement Newton's second law, we construct the free-body diagram shown in Figure 3-7 and note that the reaction force is decomposed into two components, $H1$ and $H3$, such that Force analysis diagram at point P (position of point 'P' with

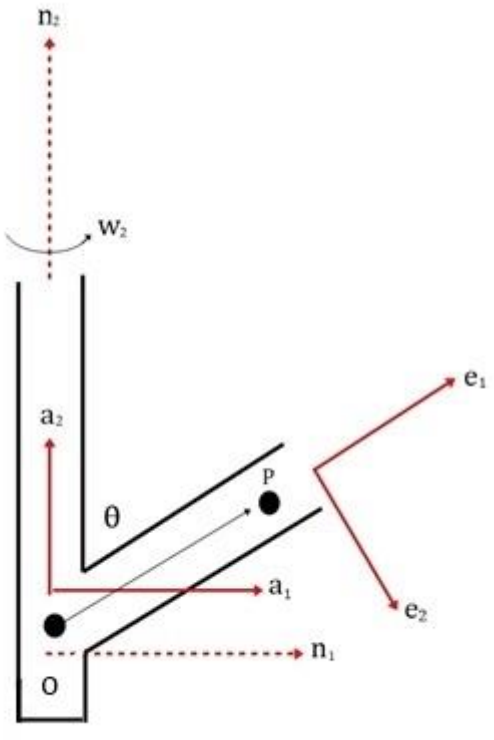

respect to 'O' in 'E' frame)

Direction $\hat{e}_1$:

$$Fe_1 = ma\hat{e}_1 \tag{3.4}$$

Figure 3.7 3-D representation of particle

$$H_1 = m \sin\theta_0 \, (g - r\omega^2 \cos\theta_0 \,) \tag{3.5}$$

Direction $\hat{e}_2$:

$$Fe_2 = \; mae_2 \tag{3.6}$$

$$\ddot{r} \; - r\omega^2 \sin\theta^2{}_0 + \mu_k N_T sgn(\dot{r}) + g\cos\theta_0 = 0 \tag{3.7}$$

Direction e_3:

$$F\hat{e}_3 = \; ma\hat{e}_3 \tag{3.8}$$

$$H_3 = -2m\,\omega\dot{r}\sin\theta_0 \tag{3.9}$$

$$\ddot{r} \; - r\omega^2 \sin\theta^2{}_0 + \mu_k \sin\theta_0 \sqrt{4\omega^2\dot{r}^2 + (g - r\omega^2\cos\theta_0)^2}\, sgn(\dot{r}) + g\cos\theta_0 = 0 \tag{3.10}$$

Using F= ma where F is the resultant force, (N), m is the mass of fertilizer particle in (kg) and a is the acceleration ($m/sec2$).

The resultant force:

$$F_T = \sqrt{F_1{}^2 + F_3{}^2} \tag{3.11}$$

In the following equations $f_{fc} = r\omega^2 \sin\theta^2{}_0$, where f_{fc} denotes the centrifugal force which are acting on the particle, r is the distance of the particle and omega is the angular velocity. $f_c = 2m\,\omega\dot{r}\sin\theta_0 sgn(\dot{r})$, where f_c is the Coriolis force, m is the mass, omega is the angular velocity, $sgn(\dot{r})$ is the linear velocity of impeller. The friction force of particle calculated as $f_f = \mu_k F_T + g\cos\theta_0$, $\mu_k$is the kinematic coefficient of friction between the fertilizer particle and pipe and g is the gravitational acceleration of the particle[60].

3.6 Theoretical Equation of Motion With no Air Resistance

Horizontal Velocity component

$$V_x = Vcos(\alpha)$$

Vertical velocity Component

$$V_y = Vsin(\alpha)$$

All the theoretical equations for motion with no air resistance have been discussed. Here I am sharing the horizontal and vertical position equations only.

These equations will use x as the particle's horizontal distance travelled, y as its height, V_x as its velocity in the x direction, and V_y as its velocity in the y direction. The general equations for projectile motion are shown below.

$$x(t) = x_0 + v_x t + \frac{1}{2} a_x t^2 \tag{3.12}$$

$$y(t) = y_0 + v_y t + \frac{1}{2} a_y t^2 \tag{3.13}$$

The only force acting on the fertilizer particle is gravity, or g, and its initial height is h_i and distance is zero. The final position equations are shown in equations 3.15 and 3.16

$$x(t) = v_x t \tag{3.14}$$

$$y(t) = h_i + v_y t + \frac{1}{2} a_y t^2 \tag{3.15}$$

When the particle touches the earth, flight is over. We can state that it occurs when the vertical distance from the ground equals 0, If we're throwing the object from a height the formula, we are left with a quadratic equation to solve:

$$t = \frac{V \times sin\alpha + \sqrt{(Vsin\alpha)^2 + 2gh}}{g}$$

The projectile's range is its overall horizontal flight distance. When the initial height deviates from 0, things become more difficult.

$$R = Vcos\alpha \times \frac{Vsin\alpha + \sqrt{(Vsin\alpha)^2 + 2gh}}{g}$$

The particle stops rising once it reaches its highest point and begins to descend. It denotes a change in its vertical velocity component from positive to negative, or, more precisely, a momentary equalization to zero.

If the particle motion starts from some height h, then formula of maximum height becomes

$$H_{max} = \frac{h + V^2 \times sin\alpha^2}{2g}$$

3.7 Motion of Fertilizer Particle with Air Drag

A fertilizer particle being projected through the air on a field is shown in Figure 3.8 At the center of mass of the particle in initial position, a Cartesian coordinate system (x, y) is attached to the field. An x-y plane is attached to the fertilizer field, with the x-axis running along the length direction, and the y-axis is perpendicular to the x-plane.

Figure 3.8 displays a free-body diagram of a particle with initial velocity. A mass m particle is travelling at a velocity of $\overrightarrow{v_0}$ leaves the spreader.

3.8 Equation of Motion with Constant Drag

Aerodynamic drag F_d, is the resistance of the air to the motion of the ball as it travels through it. The force that opposes the particle's flight direction is known as

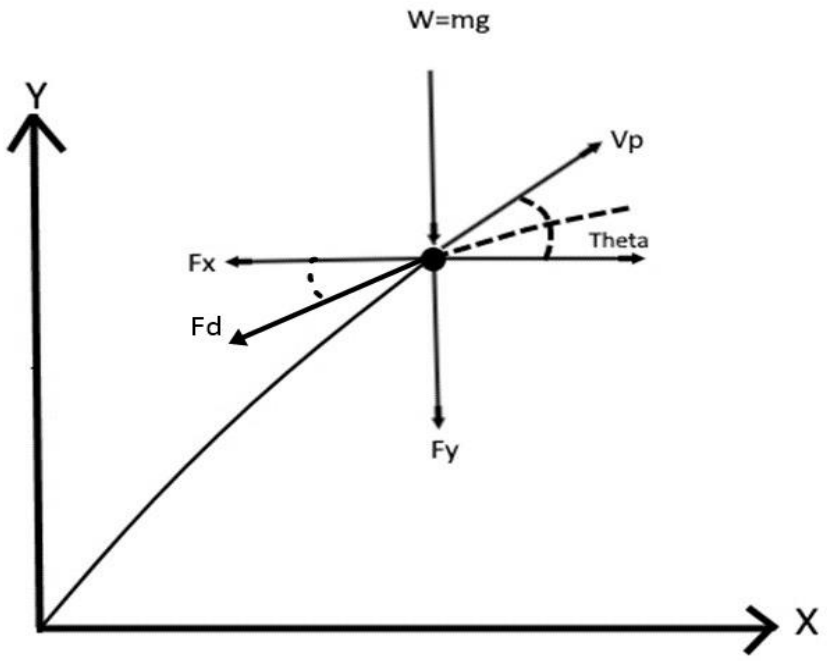

Figure 3.8: Free body diagram without air drag

aerodynamic drag. It is influenced by the air's density, the ball's cross-sectional area, its speed, and other factors like C_d the drag coefficient.[61]–[63]

With Re = 4 910 and C_d = 0.25, it is expected that the air friction will remain constant for the analysis' second section. Expressions for the motion can be derived from equations 3.16 through 3.18.

$$D = \frac{1}{2} C_D \rho A V^2$$

(3.16)

$$Re = \frac{\rho V d}{\mu}$$

(3.17)

$$\tau = \frac{m}{3\pi d \mu}$$

(3.18)

It is necessary to locate the differential equation for the x direction first. Newton's second law is depicted for the x direction in equation 3.19.

$$F_x = m a_x$$

(3.19)

Equation 3.16 can be used in place of equation 3.19 since the only force acting in the x direction, the direction opposite to the velocity is air resistance. The result is equation 3.20.

$$a_x = -\frac{C_D \rho A {V_x}^2}{2m}$$

(3.20)

The diameter of the particle can be used to express the projected area of the particle normal to the air flow. The terms of Re can be obtained by multiplying by $\frac{\mu}{\mu}$. This simplification is shown in Equation 3.21.

$$a_x = -\frac{C_D \rho \pi d \mu}{8m} V_x \frac{\rho u d}{\mu} = -\frac{C_D Re}{8} \frac{\pi d \mu}{m} V_x$$

(3.21)

Equation 3.18 may be submitted to equation 3.21 and a_x may be changed to $\frac{dt}{du}$. The complete governing equations for motion in the x direction is shown in equation 3.22.

$$\frac{dV_x}{dt} = -\frac{C_D Re}{24\tau} V_x$$

(3.22)

Next is the formulatiom of the differential equation for the y direction. Newton's second law is depicted for the y direction in equation 3.23.

$$F_y = ma_y$$

(3.23)

The velocity in the y direction is influenced by two forces: gravity and air friction. Equation 3.24 demonstrates the substitution of these two forces.

$$a_y = -\frac{C_D \rho A {V_y}^2}{m} - g$$

The complete differential equation for motion in the y direction is shown in equation 3.25.

$$\frac{dV_y}{dt} = -\frac{C_D Re}{24\tau} V_y - g$$

(3.24)

The derivatives of the position with respect to time can be expressed as V_x and V_y since these are the velocities in the x and y directions, respectively. The differential equations with constant air friction will now be solved.

$where\ -\frac{C_D R_e}{24\tau}$ is a constant,

$$\frac{dV_x}{dt} - kV_x = 0$$

(3.25)

$$\frac{dV_y}{dt} - kV_y = -g$$

(3.26)

Equation 3.28 will show the solution of equation 6-26 for V_x,

$$V_x = V_{0x} e^{kt}$$

(3.27)

By integrating and Simplifying Eq 3.28 gives

$$x(t) = -\frac{V_{0x}}{K} + \frac{V_{0x}}{k} e^{kt}$$

(3.28)

Equation 3.30 shows the equation 3.27 solved for V_y,

$$V_y = [V_{0y} - \frac{g}{k}]e^{kt} + \frac{g}{k}$$

(3.29)

By integrating and simplifying Eq 3.20 gives

$$y(t) = \frac{1}{k}\left[V_{0y} - \frac{g}{k}\right] e^{kt} + \frac{g}{k}t - \frac{1}{k}\left[V_{0y} - \frac{g}{k}\right]$$

(3.30)

3.9 Motion of Fertilizer Particle with Constant Air Drag and Downwash Thrust of Air

The third part of the analysis has been started in which we will assume that air friction is defined by the conditions in the following equations 3.32 and 3.33.

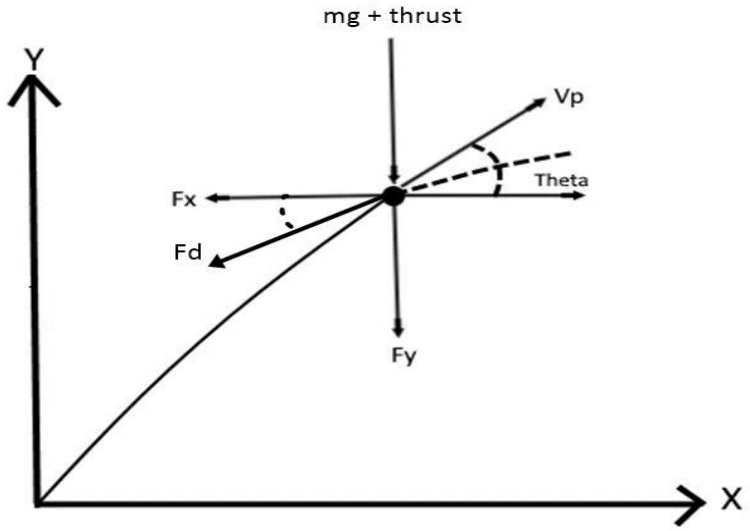

Figure 3.9 Free Body Diagram of Fertilizer Particle with thrust

$$C_d = 0.4 \quad for \quad R_e \leq 9 \times 10^4$$

(3.31)

$$C_d = 0.1 \quad for \quad R_e > 9 \times 10^4$$

(3.32)

Equations 3.34, 3.35, 3.36, and 3.27 were used to derive expressions for position and velocity.

$$x(t) = x(t - \Delta t) + \frac{\Delta t}{2}[V_x(t - \Delta t) + V_x(t)]$$

(3.33)

$$y(t) = y(t - \Delta t) + \frac{\Delta t}{2}\left[V_y(t - \Delta t) + V_y(t)\right]$$

(3.34)

$$V_x = V_x(t-\Delta t) - \frac{C_d R_e}{24\tau}\left[\frac{V_x(t-\Delta t)+V_x(t)}{2}\right]\Delta t \tag{3.35}$$

$$V_y(t) = V_y(t-\Delta t) - \frac{C_d R_e}{24\tau}\left[\frac{V_y(t-\Delta t)+V_y(t)}{2}\right]\Delta t - g\Delta t \tag{3.36}$$

We are now simplifying the equation of $v_x(t)$,

$$V_x(t) + \frac{C_d R_e \Delta t}{48\tau} V_x(t) = V_x(t-\Delta t) - \frac{C_d R_e \Delta t}{48\tau} V_x(t-\Delta t)$$

In this way,

$$V_x(t)\left[1 + \frac{C_d R_e \Delta t}{48\tau}\right] = V_x(t-\Delta t) - \frac{C_d R_e \Delta t}{48\tau} V_x(t-\Delta t)$$

After solving we are left with $v_x(t)$ on the left side:

$$V_x(t) = \frac{V_x(t-\Delta t) - \frac{C_d R_e \Delta t}{48\tau} V_x(t-\Delta t)}{\left[1 + \frac{C_d R_e \Delta t}{48\tau}\right]}$$

Simplifying the equation above:

$$V_x(t) = \frac{48\tau[V_x(t-\Delta t)] - C_d R_e \Delta t[V_x(t-\Delta t)]}{48\tau + C_d R_e \Delta t} \tag{3.37}$$

All the $V_y(t)$ terms were first moved to equation 3.28's left side to create the $V_y(t)$ equation:

$$V_y(t) + \frac{C_d R_e \Delta t}{48\tau} V_y(t) = V_y(t-\Delta t) - \frac{C_d R_e \Delta t}{48\tau} V_y(t-\Delta t) - g\Delta t$$

In this way,

$$V_y(t)\left[1 + \frac{C_d R_e \Delta t}{48\tau}\right] = V_y(t-\Delta t) - \frac{C_d R_e \Delta t}{48\tau} V_y(t-\Delta t) - g\Delta t$$

After solving we are left with $v_y(t)$ on the left side:

$$V_y(t) = \frac{V_y(t-\Delta t) - \frac{C_d R_e \Delta t}{48\tau} V_y(t-\Delta t) - g\Delta t}{[1 + \frac{C_d R_e \Delta t}{48\tau}]}$$

Simplifying the equation above:

$$V_y(t) = \frac{48\tau\left[V_y(t-\Delta t)\right] - C_d R_e \Delta t\left[V_y(t-\Delta t)\right] - 48\tau g\Delta t}{48\tau + C_d R_e \Delta t} \quad (3.38)$$

$$V_{air} = \sqrt{\frac{thrust\ of\ one\ propeller}{\rho_{air} * A}}$$

$$F_{Air\ thrust} = 0.5 * C_d * \rho_{air} * A_p {V_{air}}^2$$

Downwash Acceleration = $F_{Air\ thrust}/m_p$

Chapter 4 Experimental Study

4.1 Introduction

In this experiment lab and field test were conducted, two different types of fertilizers were used during lab and static field test. In first phase UREA fertilizer was used and in 2nd phase DAP fertilizer was used. The main objective of this experiment to evaluate the error produced from theoretical and real time application of fertilizer. The primary goal of this field test, in the context that has been discussed, was testing the integration of various hardware and software components into an automatic control system for drone base manual adjustable variable rate fertilizer application, incorporated into a conventional seeding-fertilizing equipment, at the prototype level, in a small testing area of crop, to assess the error generated by the system for different distances of resolution along the path of the fertilizer application. The key justification for using such a tiny area is that a specialty slow-release fertilizer, which is highly expensive and needs very precise rates ranging between 20 and 150 kg/ha, roughly, was assessed.

4.2 Physical Properties of Granular Fertilizer

In this experiment granular Urea Fertilizer and Dap was used, 46% was nitrogen content was present. The urea particles diameter was 1 to 3.25 mm, So the average

Figure 4.1 (a) Urea Fertilizer (b) DAP Fertilizer

particle diameter was 2mm, the bulk density was taken 2000 kg/m^3. Table 4.1 show the diameter were bulk density of urea fertilizer.

Table 4-1 Urea Fertilizer Specifications

Sr. No	Urea Fertilizer Particle diameter mm	Bulk Density Kg/m^3
1.	1.00	1200
2.	1.25	1400
3.	1.50	1600
4.	1.75	1800
5.	2.00	2000
6.	2.25	2200
7.	2.50	2400
8.	2.75	2600
9.	3.00	2800
10.	3.25	3000

4.3 Granular Fertilizer Spreader

In this experiment centrifugal fertilizer spreader was used, the test was carried out at sports ground of College of Electrical and Mechanical Engineering, NUST, Rawalpindi. Flow rate adjustment was done with manual variable rates, flow rate adjustment was shown in figure 4.2

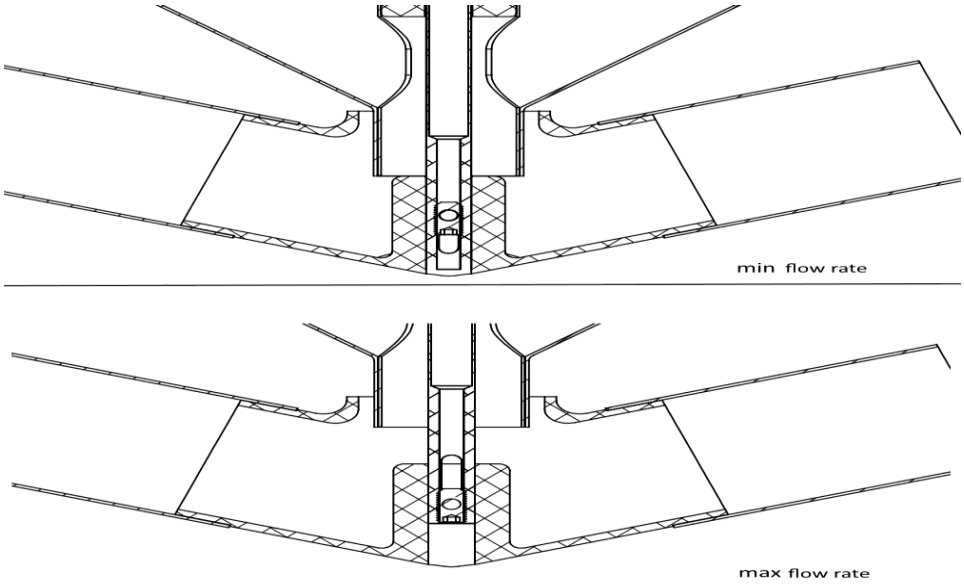

Figure 4.2 Maximum and Minimum flow rate Adjustment

4.4 Experimental Instruments Used

Fertilizer Spreader, Tachometer, Dc Motor controller, Measuring Tape, Impeller Battery and motor.

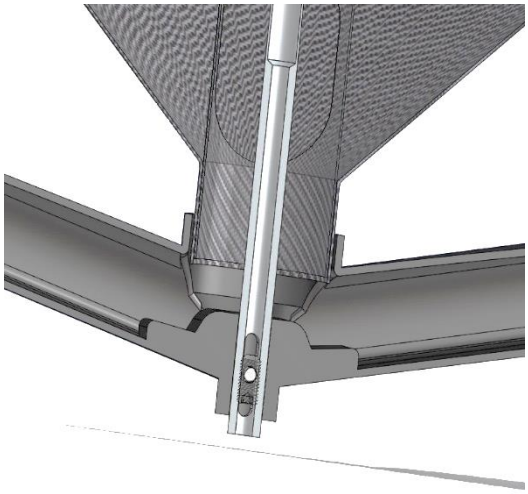

Figure 4.3 Impeller Section view

Chapter 5 Computer simulation

5.1 Introduction

Computer simulation is the process of using a computer to simulate the behavior of another system to reflect the dynamic reactions of a first system. A simulation employs a computer software such as MATLAB that acts as a mathematical model or description of a real system. Equations that replicate the functional relationships seen in the actual system make up this model. The results are supplied as data, and when the program is executed, the resulting mathematical dynamics create an analogue of the behavior of the real system. A computer-graphics image that depicts dynamic processes in an animated sequence can also be used as a simulation.

Computer simulations are used to explore how things or systems respond dynamically to situations that are difficult or unsafe to apply in the actual world. For instance, a mathematical model that considers factors like heat, velocity, and radioactive emissions can be used to explain a nuclear bomb. The model can then be modified to account for changes in specific variables, such as the volume of fissionable material that caused the explosion, using additional mathematical equations. Simulations are particularly helpful in enabling observers to quantify and forecast how changing a single system component may affect the functioning of the entire system.

we are going to use MATLAB for computer simulation and to study the motion of particle inside impeller and the trajectory of fertilizer particle and effect of variable initial velocity, constant air drags, variable drag over its path and downwash air. Then we will compare the theoretical results with computer simulated results to get optimize angle and optimize initial velocity to get maximum output.

5.2 Motion of Single Fertilizer Particle Inside Impeller

When fertilizer seed fall under the action of gravity in non-inertial reference system they will ejected from impeller under the action of centrifugal force. When the fertilizer particles move in impeller, they will face frictional forces from the impeller, thrust from pipe and Coriolis force. Fertilizer particle ejected from impeller and move inside pipe. The kinematic analysis of the fertilizer particle following impact to their initial velocity and angle of impeller [59].

We can write the position, velocity, and acceleration of point P with respect to point O measured in the inertial frame as follows:

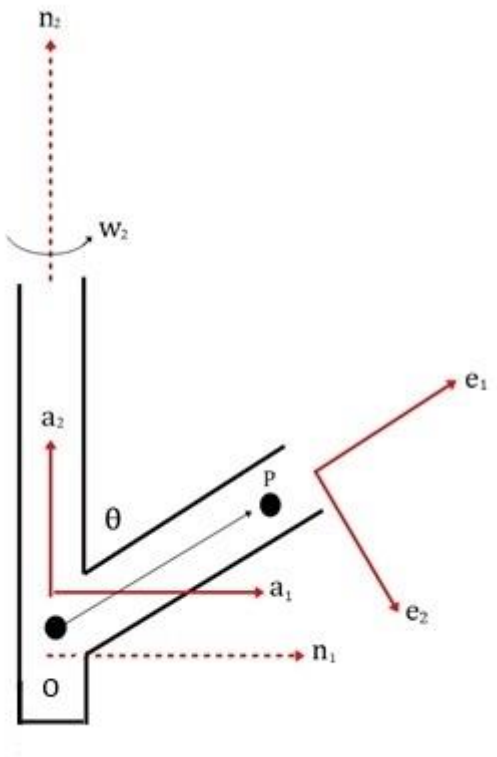

Figure 5-1 Motion of particle inside impeller

$$Position = r\hat{e}_2 \tag{5.1}$$

$$Velocity = \dot{r}\hat{e}_2 - r\omega \sin\theta_0\, \hat{e}_3 \tag{5.2}$$

$$Acceleartion = -\mathrm{r}\omega^2 \sin\theta_0 \cos\theta_0\, \hat{e}_1 + (\ddot{\mathrm{r}} - \mathrm{r}\omega^2 \sin{\theta_0}^2)\hat{e}_2 - 2\dot{r}\omega \sin\theta_0\, \hat{e}_3 \tag{5.3}$$

$$\ddot{r} - r\omega^2 \sin{\theta_0}^2 + \mu_k \sin\theta_0 \sqrt{4\omega^2\dot{r}^2 + (g - r\omega^2 \cos\theta_0)^2}\, sin(\dot{r}) + g\cos\theta_0 = 0 \tag{5.4}$$

Using equation 5-4 we can determine position, radial velocity, and radial acceleration at different rpm. Table 5.1 show the initial condition for kinematic analysis of Granular Urea Fertilizer particle motion inside impeller.
Where $\boldsymbol{v_t}$ is the Tangential Velocity *and* $\boldsymbol{v_x}$ is the radial velocity given as

$$\boldsymbol{v_t} = \boldsymbol{r} \times \boldsymbol{\omega}$$

$$\boldsymbol{v_x} = r\omega^2 \sin\theta_0{}^2 - \mu_k \sin\theta_0 \sqrt{4\omega^2\dot{r}^2 + (g - r\omega^2 \cos\theta_0)^2}\, sin(\dot{r}) - g\cos\theta_0$$

(5.5)

By using MATLAB code is in Appendix A for position, radial velocity, and at different RPM and initial angles is 25 degrees. Figures 5.2, 5.3 and 5.4 show the distance versus time and radial velocity versus time plot. In figure 5.2 shows that the particle does not come out of spreader due to low velocity. Figure 5.4 shows the *rpm* at which particle gains its maximum radial velocity.

Table 5-1 Initial condition for Kinematic analysis

Length of Impeller $(\boldsymbol{m})$	***Kinematic Visco sty*** $(\boldsymbol{\mu_k})$	***RPM***	***Position*** $(\boldsymbol{m})$	$\boldsymbol{v_x}$ $(\boldsymbol{m/sec})$	$\boldsymbol{v_t}$ $(\boldsymbol{m/sec})$	$\boldsymbol{v_{resultant}}$ (m/sec)
0.155	0.3	50	0.0062	0.00	0.81	0.811578102
0.155	0.3	100	0.01	0.00	1.62	1.6231
0.155	0.3	150	0.0204	0.51	2.43	2.4868
0.155	0.3	200	0.0419	1.75	3.25	3.6888
0.155	0.3	250	0.0801	4.40	4.06	5.9822
0.155	0.3	300	0.155	9.87	4.87	11.0043
0.155	0.3	350	0.155	12.12	5.68	13.3850
0.155	0.3	400	0.155	14.15	6.49	15.5684
0.155	0.3	425	0.155	14.72	6.49	16.0922

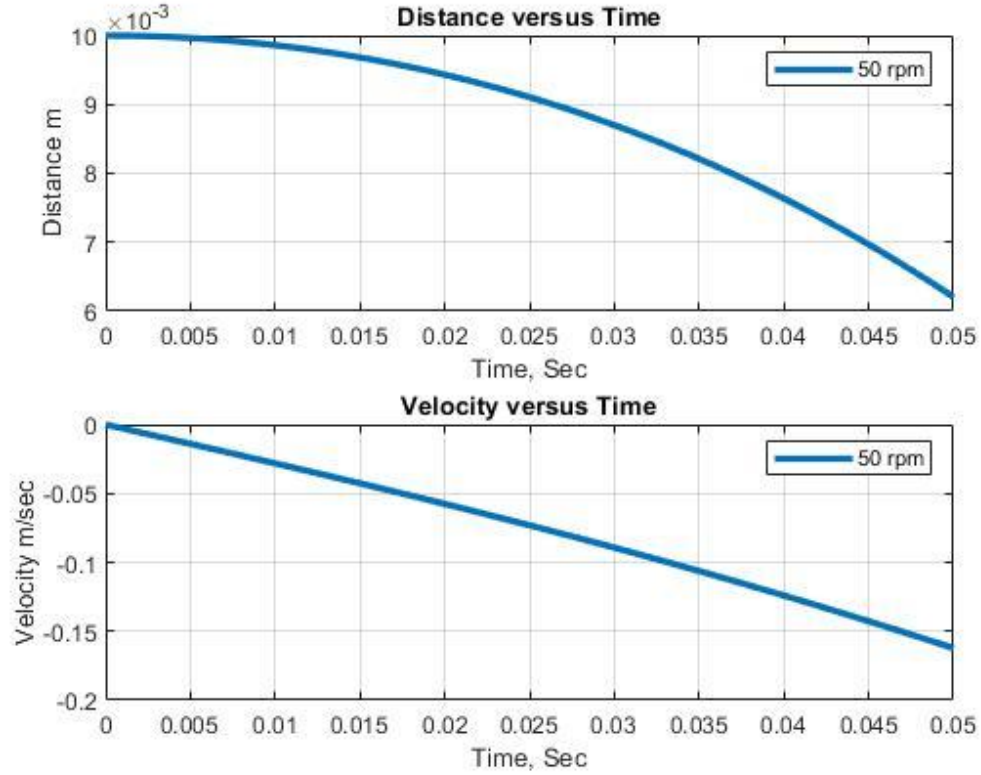

Figure 5-2 Distance, Radial Velocity vs time Graphs for 50 rpm

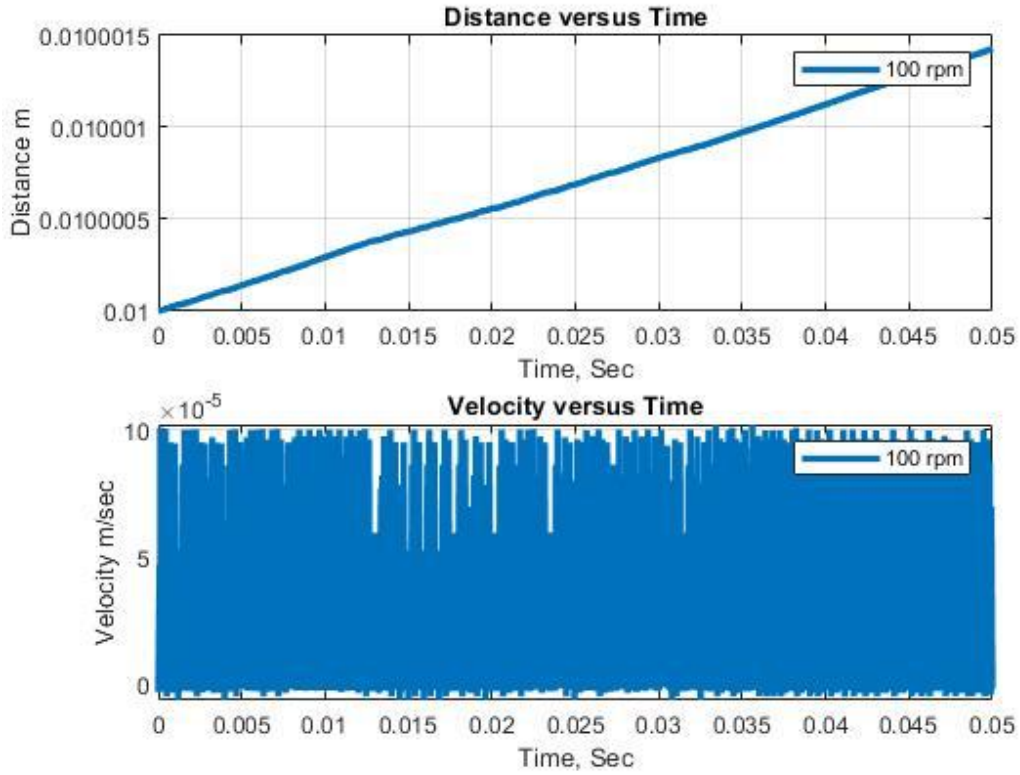

Figure 5-3 Distance, Radial Velocity vs time Graphs for 100 rpm

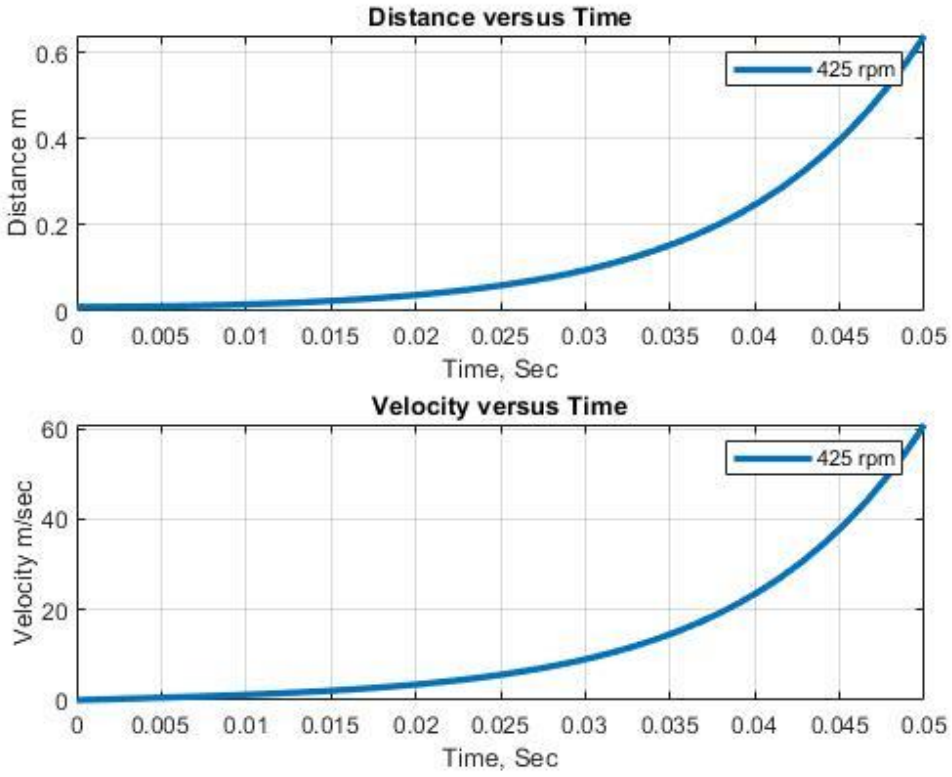

Figure 5.4 Distance, Radial Velocity vs time Graphs for 425rpm

5.3 Fertilizer Particle Motion Outside Impeller

When fertilizer particle comes out of impeller the particle follows a trajectile motion under the action of gravity. Drag force and upward air thrust comes into play and change the trajectory of particle.

5.4 Effect of Initial Angle on Particle's Trajectory

Table 5.2 Initial condition for a projectile motion at different angles

Parameter	**Values**									
Initial Height (m)	2									
Initial Velocity (m/s)	16.09									
Initial Angles Θ (°)	0	5	10	15	20	25	30	35	40	45
Time Spans (sec)	0.63	0.79	0.98	1.18	1.41	1.63	1.85	2.07	2.28	2.48
Max Range R_{max} (m)	11.3	15.0	18.5	22.4	26.3	29.7	32.8	34.6	35.8	36.2
Max Height H_{max} (m)	2	2.3	6.15	8.5	10.9	13.4	14.9	15.4	16.7	17

We have studied the effect of changing the initial velocity now we are going to study the effect of changing the initial angle on our Fertilizer projectile motion, this will help us to find the optimal angle. MATLAB code is in Appendix B.

The dynamic simulation of a fertilizer particle projectile motion with different initial angles is shown in Figure 5.5 The initial parameters are shown in

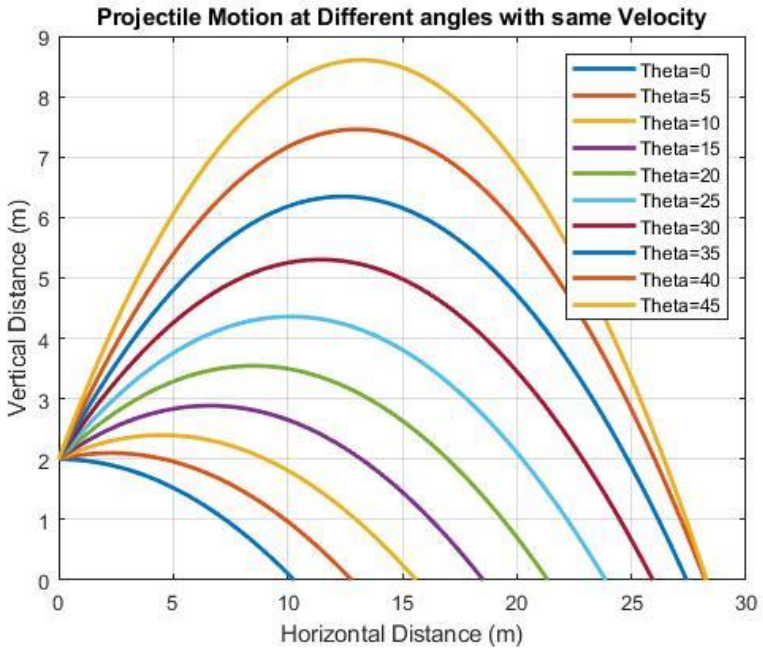

Figure 5.5 Projectile motion at different angles Horizontal and Vertical Distance

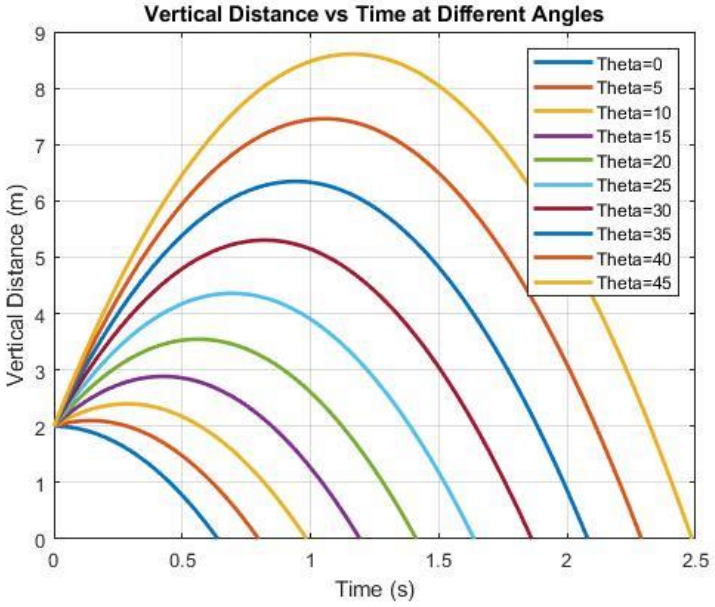

table 5.2

.

Figure 5.6 Height Vs Time at different angles

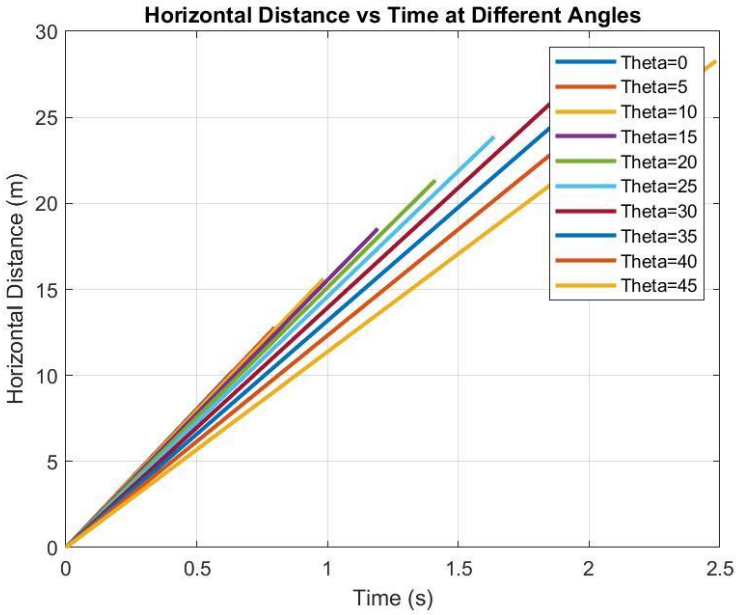

Figure 5.7 Distance Vs Time at different angles

Due to their inertia, particles with a higher beginning velocity go farther. The flight of particle is affected by changing initial angle or initial velocity. First, we will discuss the effect of initial velocity on the flight of particles projectile motion and how it effects the maximum range and maximum height.

By choosing eleven sets of beginning velocities and simulating times, the MATLAB code Appendix C of particles projectile motion is developed.

The dynamic simulation of a fertilizer particle projectile motion is shown in Figure 5.9 to 5.12 The initial parameter with variable initial velocities is given in table 5.4.

Table 5.3: condition for a projectile motion at different angles

Parameter	**Values**						
Initial Height (m)	2						
Initial Angle Θ (°)	25						
Initial Velocities (m/s)	0.81	1.62	2.48	3.69	5.98	11	16.09
Time Spans (sec)	0.67	0.72	0.77	0.85	1	1.41	1.86
Max Range R_{max} (m)	25.93						
Max Height H_{max} (m)	5.3052						

The flying height (vertical distance) vs (horizontal distance) range are shown in the figure 5.8. It has been discovered that the Particle flies higher and further when the initial velocity is higher. Two important elements that are addressed in this Chapter are the maximum projectile height H and maximum projectile range R. The max distance a particle covers horizontal direction from starting point till it hits the ground is called Range R_{max}. The maximum projectile height H is defined as the distance between the initial point and the highest point H_{max}. According to Fig. 5.9, the distance between the starting point and the point where particle hits the ground occurs at maximum velocity 16.09m/s which comes out to be 25.93 m. All the values are shown in table 5.2.

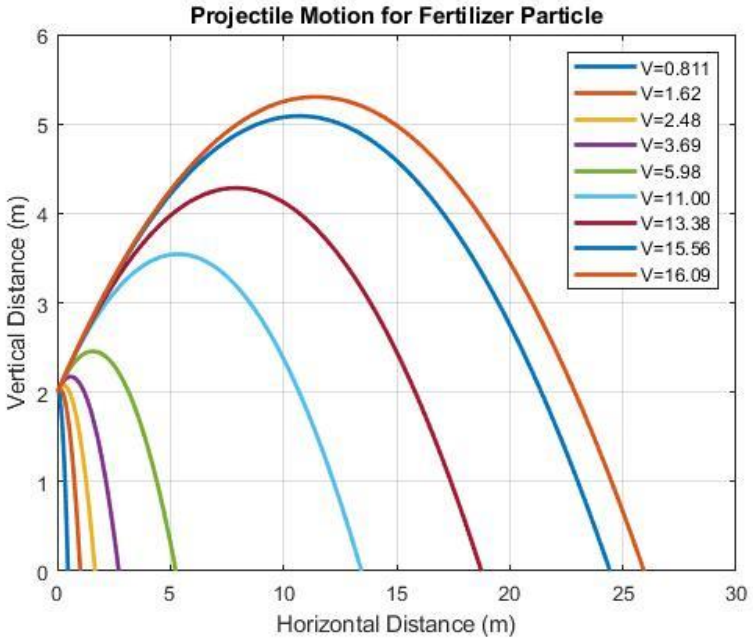

Figure 5-8 Projectile motion at different Velocity

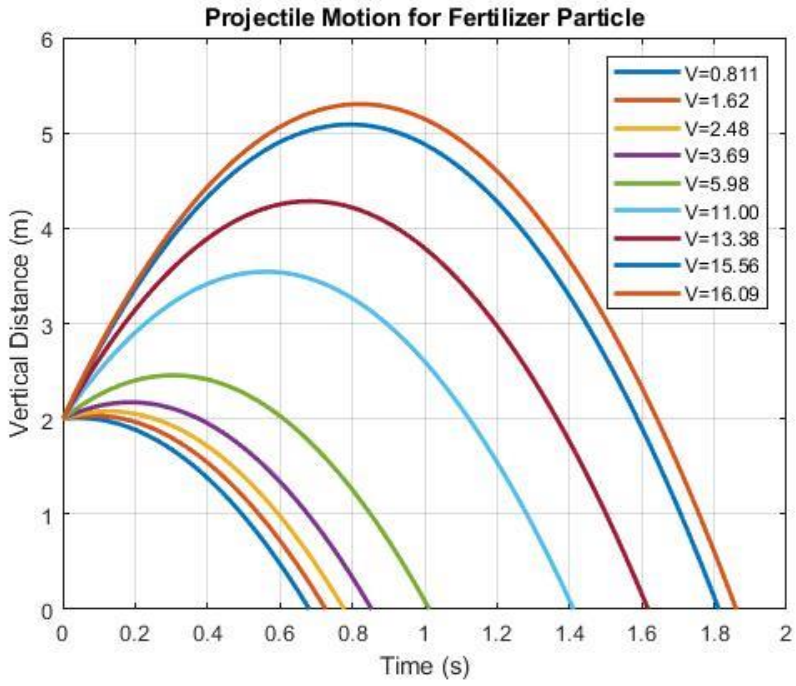

Figure 5.9 Vertical Distance vs Time

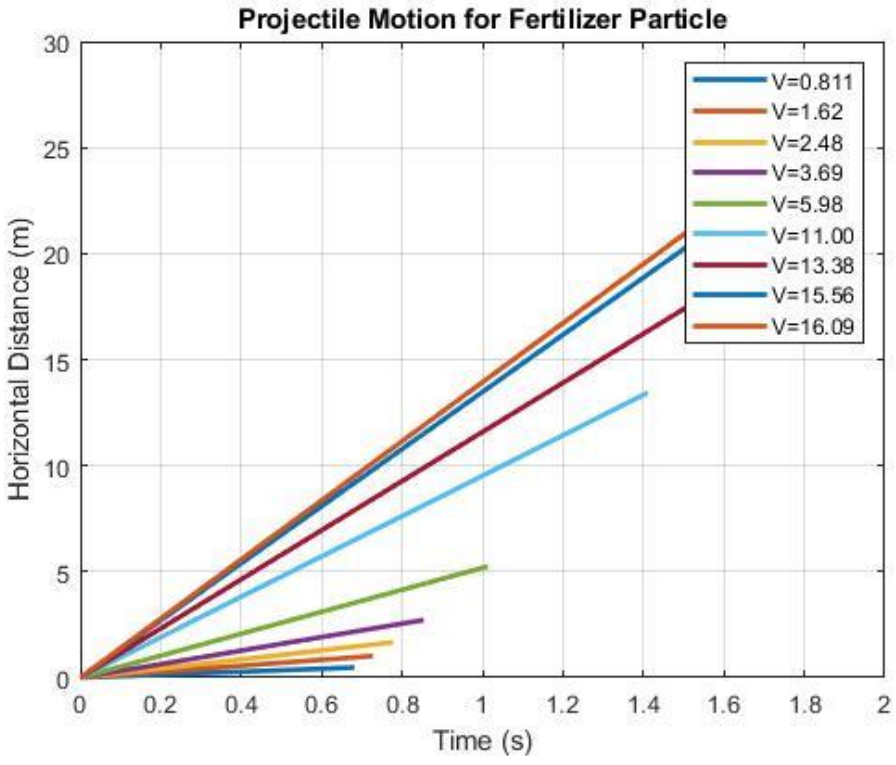

Figure 5.10 Horizontal Distance vs Time

All the theoretical equations for motion with no air resistance have been discussed. Here I am sharing the horizontal and vertical position equations only.

These equations will use $x(t)$ as the particle's horizontal distance travelled, $y(t)$ as its height, V_x as its velocity in the x direction, and V_y as its velocity in the y direction the MATLAB code Appendix D of particles projectile motion is developed. The general equations for projectile motion distances are shown in equations -1 and 6-2The only force acting on the fertilizer particle is gravity, or g, and its initial height is h_i and distance is zero. The final position equations are shown in equations 5.5 and 5.6

$$x(t) = u_0 t \tag{5.6}$$

$$y(t) = h_i + v_0 t + \frac{1}{2} a_y t^2 \tag{5.7}$$

With these equations, MATLAB in appendix D was used to plot the path of the Fertilizer Particle. Figure 5.7 shows the path of the Particle with no air friction. Initial values for projectile motion are shown in Table 5.6

Table 5.4 Physical parameter with no air drag

Parameter	**Values**
Initial Height (m)	2
Initial Velocity (m/s)	16.09
Initial Angles Θ (°)	25
Max Range R_{max} (m)	23.76
Max Height H_{max} (m)	4.35

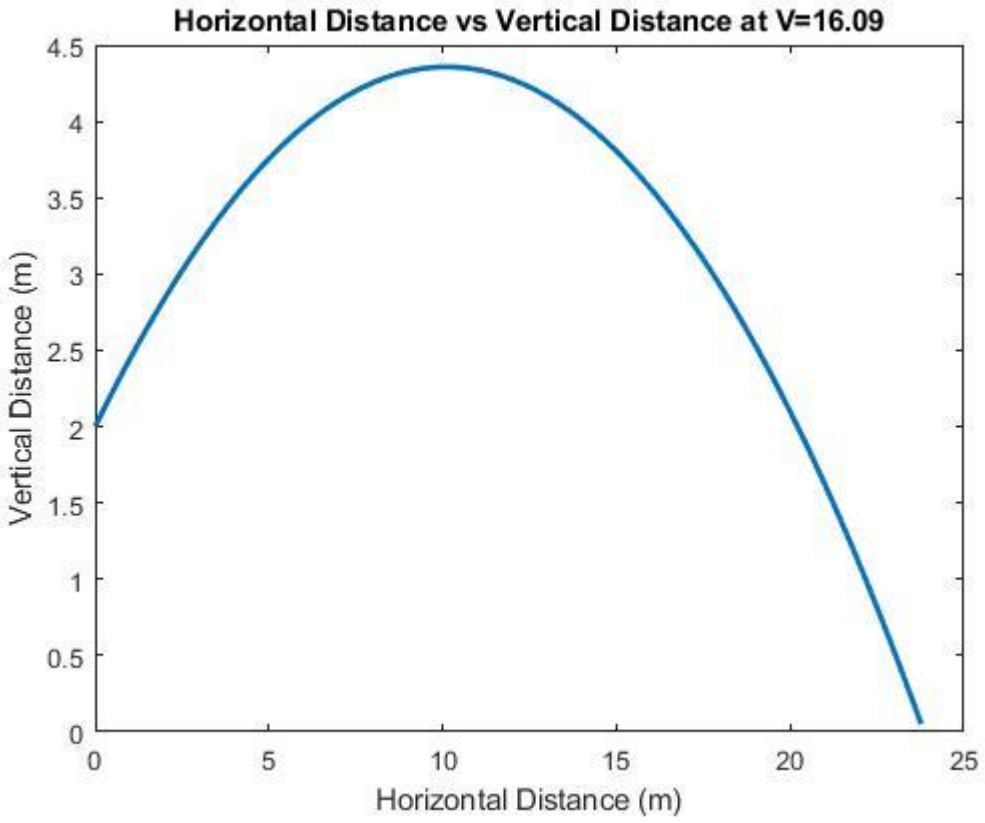

Figure 5.11 Projectile motion with no air drag

5.5 With Constant Air Drag

Aerodynamic drag, or F_d, is the resistance of the air to the motion of the ball as it travels through it. The force that opposes the particle's flight direction is known as aerodynamic drag. It is influenced by the air's density, the ball's cross-sectional area, its speed, and other factors like C_d the drag coefficient.[61]–[63]. Following are the equations for projectile motion by considering the effect of Drag Force the MATLAB code Appendix E of particles projectile motion is developed.

$$V_x = V_{0x} e^{kt} \tag{5.8}$$

$$x(t) = -\frac{V_{0x}}{k} + \frac{V_{0x}}{k} e^{kt} \tag{5.9}$$

$$V_y = [V_{0y} - \frac{g}{k}]e^{kt} + \frac{g}{k} \tag{5.10}$$

$$y(t) = \frac{1}{k}\left[V_{0y} - \frac{g}{k}\right] e^{kt} + \frac{g}{k} t - \frac{1}{k}\left[V_{0y} - \frac{g}{k}\right] \tag{5.11}$$

Where k is a constant equals to $-\frac{C_D R_e}{24\tau}$

Initial values with Re = 4.910 and C_d = 0.30, is shown in table 5.5 and for these values it is expected that the air friction will remain constant for the analysis.

Table 5.5 Initial condition and physical property

Parameter	Values
Diameter of particle (m)	0.002
Density of Particle (kg/m^3)	2000
Density of Air (kg/m^3)	1.18
Temperature in degree	25
Initial Height (m)	2
Initial Velocity (m/s)	16.09
Initial Angles Θ (°)	25
Coefficient of Drag in x C_d	0.30
Coefficient of Drag in y C_d	0.3
Reynolds Number Re	4.910
Max Range R_{max} (m)	11.29
Max Height H_{max} (m)	3.2

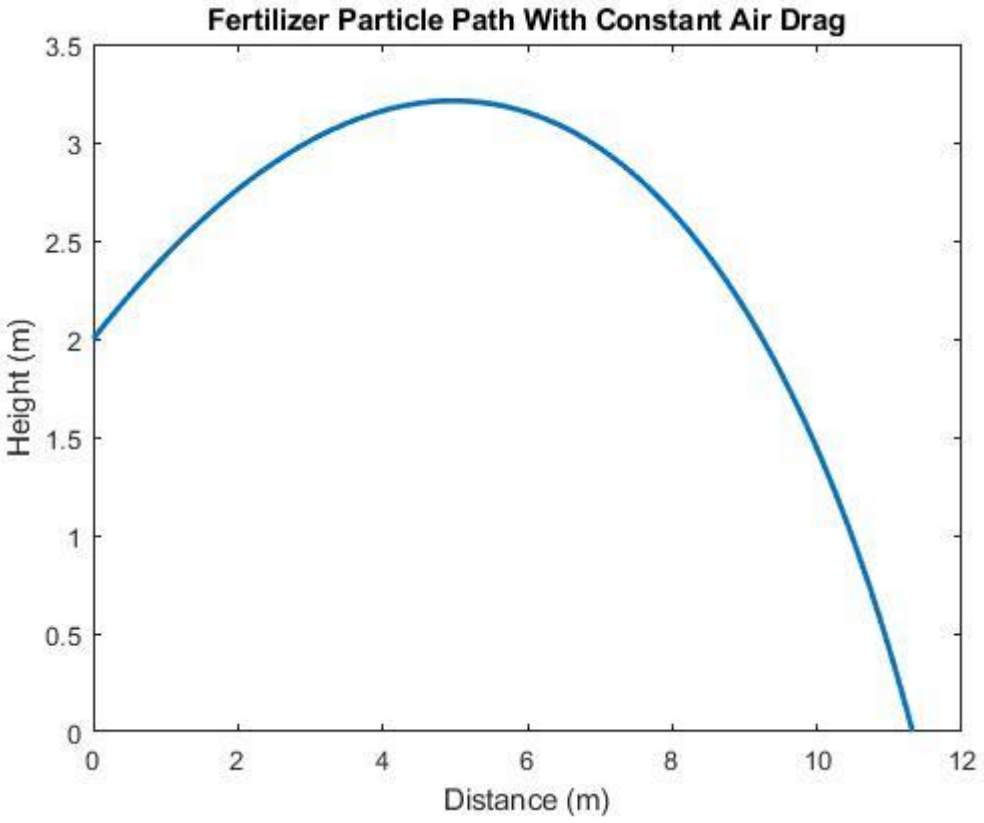

Figure 5.112 Projectile motion at Constant Drag

The third part of the analysis has been started in which we will assume that air friction is a function of velocity and is constrained by following values

$$C_D = 0.4 \quad for \quad R_e \leq 9 \times 10^4$$
$$C_D = 0.1 \quad for \quad R_e > 9 \times 10^4$$

$$x(t) = x(t - \Delta t) + \frac{\Delta t}{2}[v_x(t - \Delta t) + v_x(t)] \tag{5.12}$$

$$y(t) = y(t - \Delta t) + \frac{\Delta t}{2}\left[v_y(t - \Delta t) + v_y(t)\right] \tag{5.13}$$

$$V_x = \frac{48\tau[v_x(t - \Delta t)] - C_D R_e \Delta t[v_x(t - \Delta t)]}{48\tau + C_D R_e \Delta t} \tag{5.14}$$

$$V_y = \frac{48\tau\left[v_y(t - \Delta t)\right] - C_D R_e \Delta t\left[v_y(t - \Delta t)\right] - 48\tau g \Delta t}{48\tau + C_D R_e \Delta t} \tag{5.15}$$

MATLAB coding were employed using equations 5.11-5.14. Both approaches produced the same outcome, as demonstrated in figure the MATLAB code Appendix F.

Table 5-6 Initial condition and physical property for Velocity at variable drag

Parameter	**Values**
Diameter of particle (m)	0.002
Density of Particle (kg/m^3)	2000
Density of Air (kg/m^3)	1.18
Temperature in degree	25
Initial Height (m)	2
Initial Velocity (m/s)	16.09
Initial Angles Θ (°)	25
Max Range R_{max} (m)	17.35
Max Height H_{max} (m)	3.96

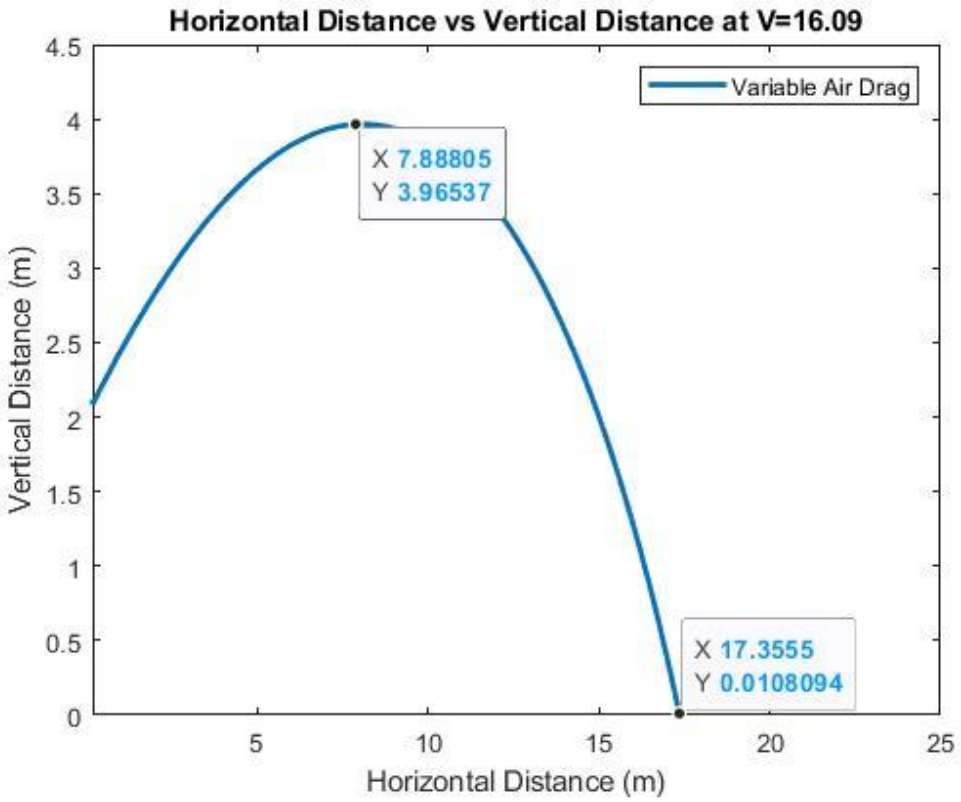

Figure 5.13 Projectile Motion at Variable drag

5.6 Downwash Air Effect

The fourth part of the analysis has been started in which we will consider the downwash air thrust of Aerial fertilizer spreader, the MATLAB code Appendix G.

- Downward Air Wash
- $V_{air} = \sqrt{\frac{thrust\ of\ one\ propeller}{\rho_{air} \times A}}$
- Downwash Air Force
- $F_{Air\ thrust} = 0.5 * C_D * \rho_{air} * A_p {V_{air}}^2$

  Downwash Air Acceleration
- Downwash Acceleration = $F_{Air\ thrust}/m_p$

$$x(t) = x(t - \Delta t) + \frac{\Delta t}{2}[v_x(t - \Delta t) + v_x(t)] \tag{5.12}$$

$$y(t) = y(t - \Delta t) + \frac{\Delta t}{2}\left[v_y(t - \Delta t) + v_y(t)\right]$$

(5.13)

$$V_x = \frac{48\tau[v_x(t - \Delta t)] - C_D R_e \Delta t[v_x(t - \Delta t)]}{48\tau + C_D R_e \Delta t}$$

(5.14)

$$V_y = \frac{48\tau\left[v_y(t - \Delta t)\right] - C_D R_e \Delta t\left[v_y(t - \Delta t)\right] - 48\tau(g + \text{Downwash Acceleration}) + \Delta t}{48\tau + C_D R_e \Delta t}$$

(5.14)

Table 5-7 Initial condition and physical property for downwash air drag

Parameter	Values
Diameter of particle (m)	0.002
Density of Particle (kg/m^3)	2000
Density of Air (kg/m^3)	1.18
Temperature in degree	25
Initial Height (m)	2
Initial Velocity (m/s)	16.09
Initial Angles Θ (°)	25
Max Range R_{max} (m)	14.45
Max Height H_{max} (m)	3.60

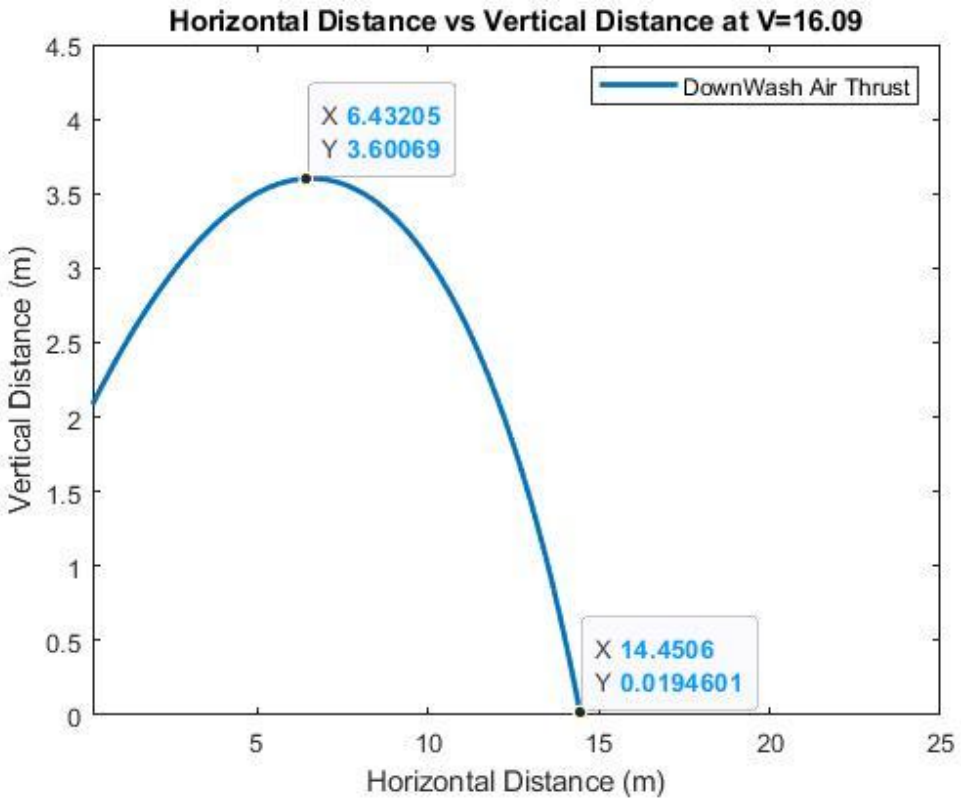

Figure 5.14 Projectile motion under Air Downwash Thrust effect

5.7 Trajectory Comparison of all Velocities

The fifth part of the analysis has been started in which we will consider the downwash air thrust of Aerial fertilizer spreader, the MATLAB code Appendix H.

Table 5.8 Comparison of all projectile motion

	Max Height H_{max} (m)	**Max Range R_{max} (m)**
With no Air Drag	4.35	23.76
With Constant Air Drag	3.2	11.23
Drag as function of Velocity	3.96	17.35
Downwash Air Thrust	3.60	14.45

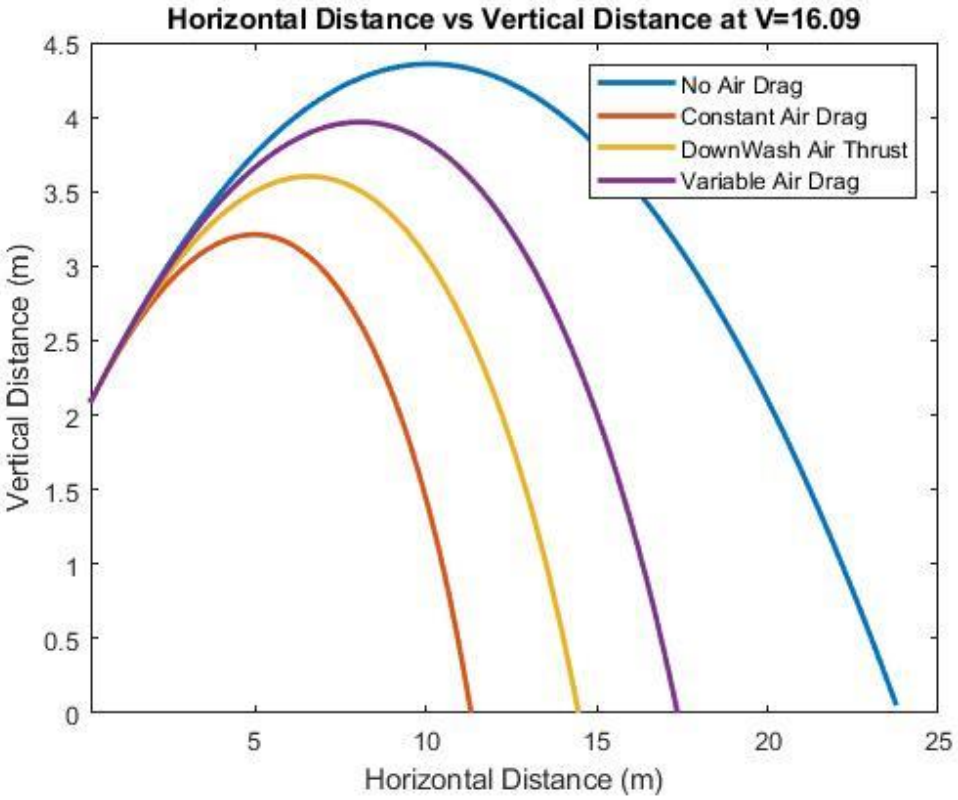

Figure 5.15 Comparison of Projectile motion

Chapter 6 Conclusion and Future work

6.1 Conclusion

For effective agriculture analysis, this thesis introduces mathematical explanation, optimization of model and trajectory, and virtual simulation of a fertilizer particle. To simulate the spatial kinematics and dynamics of a fertilizer particle, the research combines mechanics, mathematics, and computer engineering. For the complete dynamic simulation of fertilizer particle motion, a foundation is established. Literature review, Mathematical explanation, Model development, Experimental Study, trajectory optimization using computer simulation are the five topics covered in chapters two through five. Each of these stands alone and emphasizes a unique characteristic of fertilizer spreader dynamics and kinematics. The thesis makes explicit reference to the problems, objectives, methods, and key findings. Strong references are used to support the fundamental modelling equations, and their physical significance is made explicit.

In Chapter 2, the articles connected to the earlier research are introduced. The methods used in earlier works have been discussed, and each one's key outcomes have been emphasized. to make it easier for the readers to understand how the subject of this thesis compares to the current work. Discussions and comparisons with newly published material are made regarding the precise contributions of the pieces in this volume. Future research is recommended along with a summary of some key findings.

Mathematical Explanation and model Development

A spatial two-dimensional body dynamics model of a fertilizer particle has been created in Chapter 2. The particle motion within spreader is explained with the effect of initial angle and rpm at which the spreader is rotating. When the particle leaves the spreader the effect of aerodynamic drag and gravity were included in the model. The study's primary focus was on examinations of aerodynamic properties.

A 3D model of fertilizer spreader is developed using solid works and is fabricated suing 3D modelling. A hexacopter drone is selected and spreader is attached to the drone for experimentation.

6.2 Experimental Study

For field test we have tested our fertilizer spreader at NUST College of EME, Sports Ground and results were noted.

6.3 Design Optimization

To forecast the target of a fertilizer, an optimization technique has been suggested. The components of aerodynamic drag, the upthrust of air, and gravity are all included in the equations of motion. The design objective has been expressed as mathematical equations with the design variables and design restrictions to optimize the moving trajectory. This model can direct a direct optimization by capturing the simultaneous distance between a ball and target. In this way, the ideal course can be found for fertilizer spreader.

An illustration of the application of the optimization design method on the fertilizer particle in Chapter 5. The outcomes show how a spreader must regulate the particle trajectory's beginning conditions to get a favorable result. It is concluded that the particles motions can be visualized visually, numerically measured, and parametrically optimized by modelling, simulation, and optimization. The outcome demonstrates that for the particle to hit the target, the most effective combination of the design parameters is initial velocity $V_0 = 16.09\, m/s$, initial projectile angle 25. The approach is therefore helpful for tracking the trajectory and enhancing the initial parameters.

6.4 Future Work

This thesis is significant to guide to design and development of Aerial fertilizer spreader, which have significant in agricultural engineering domain. In this thesis we have analyze and simulate the projectile motion of fertilizer particle for optimizing the trajectory and accurate position. Improved through this model further investigation. Mathematical model can be extending the current equation of motion by adding more factor, such as Coriolis effect. Prepare map using pix4d software which are helpful for interfiled variability.

In future, it is recommended that , a geographical map can be installed within the drones that can be used for exact throw of particles. Moreover , its mathematical model can be improved to increase the stability of drones and further spread of water partricles in the field.

Appendix A

```
function dx=f_(t,x)
global mu
global omega
global theta
global g
x1=x(1);
x2=x(2);
dx1=x2;
% velocity on that points
dx2= x1*(omega^2)*sin(theta)^2 - (mu*sin(theta)*sqrt((4*(omega^2)*(x2^2))+(g-
x1*(omega^2)*cos(theta))^2))*sign(x2) - g*cos(theta);
dx=[dx1;dx2];
end
```

Appendix B

```
close all
clc
clf
global mu
global omega
global theta
global g

mu=0.30;
g=9.81;
theta=25*pi/180;
omega=425;
%initial condition
x0=[0.01 0]; % initial displacment=0,
%solve ODE
[t,result]=ode45(@f_,[0 0.05],[x0]);
x1 = result(:,1);
x2 = result(:,2);
subplot(2,1,1)

figure(1)
subplot(2,1,1)
plot(t,x1,'LineWidth',2.5)
title('Distance versus Time')
xlabel('Time, Sec')
ylabel('Distance m')
```

```
legend('425 rpm')
hold on
grid on
figure(1)
subplot(2,1,2)
plot(t,x2,'LineWidth',2.5)
title('Velocity versus Time')
xlabel('Time, Sec')
ylabel('Velocity m/sec^2')
legend('425 rpm')
hold on
grid on
```

Appendix C

```
%% Position of Particle in x and Y At different velocity and Same angle WITHOUT
DRAG on same figues.
% v = [0.811578102 1.623156204 2.486843883 3.688849066 5.982279689
%      11.00439294 13.38506684 15.56845134 16.09223616 ];


 %initial velocity, m/s
 v=[16.09];

g = 9.8;% m/sec^2
h =2; %initial height is 3m
% theta = (0:5:45)*(pi/180); % angle in radians
theta=pi/6;
dt=0.01;

t_total = zeros(length(v), length(theta));
Tmax = zeros(length(v), length(theta));
H_max = zeros(length(v), length(theta));
Range = zeros(length(v), length(theta));
% t_total = zeros(length(v));
% Tmax = zeros(length(v));
% Range = zeros(length(v));
% H_max = zeros(length(v));
% for ii=1:length(v)
% t_total=
k = 1;

format short g;
for jj = 1:length(v)
    for ii = 1:length(theta)

      t_total(jj,ii) = (v(jj)*sin(theta(ii))+sqrt((v(jj)*sin(theta(ii)))^2 + (2*g*h)))/g;
%Time of flight: t = [Vy + ?(Vy² + 2 * g * h)] / g
      Tmax(jj,ii) = v(ii)*sin(theta(ii))/g;%time for maximum height
      vx = v(jj)*cos(theta(ii)); % Velocity in X-Direction Vx = V * cos(?)
      vy_initial = v(jj)*sin(theta(ii));%initial velocity on launch Vy = V * sin(?)
```

```
time_range = (0:0.01:t_total(jj,ii)); % Time Span
if time_range(end) ~= t_total(jj,ii)
   time_range(end+1) = t_total(jj,ii);
end
% Total of Projectile motion

vy = vy_initial-(g*time_range); % Velocity of fertilizer parrticle when starts to move ertical velocity can be expressed as Vy – g * t.

vy_final = vy_initial-(g*t_total(jj,ii)); % Velocity when fertilizer particle hit the ground ertical velocity can be expressed as Vy – g * t.

Y = h + (vy_initial*time_range) - 0.5*(g*time_range.^2); %Vertical distance from the ground is described by the formula y = h + Vy * t – g * t² / 2, where g is the gravity

Y = round(Y*100000)/100000;

X = vx*time_range; %Horizontal distance traveled can be expressed as x = Vx * t, where t is the time.
V = sqrt(vy.^2+vx.^2); %c = ?(b²+a²)
H_max(jj,ii) = ((vy_initial^2)/(2*g))+ h;% total vertical distance, initial height is h hmax = h + Vy² / (2 * g)
Range(jj,ii) = vx*t_total(jj,ii) ; %Total hotizontal distance
sz=size(time_range);
a= ones(sz);
vx=vx*a;
figure(k)
plot(time_range,vx,'LineWidth',2);
grid on;
title('Projectile Motion for Fertilizer Particle');
xlabel('Time (s)');
ylabel('horizontal velocity');

legend('V=0.811','V=1.62','V=2.48','V=3.69','V=5.98','V=11.00','V=13.38','V=15.56','V=16.09');
 hold on;
figure(k+1)
plot(time_range,vy,'LineWidth',2);
grid on;
title('Projectile Motion for Fertilizer Particle');
xlabel('Time (s)');
ylabel('vertical velocity');

legend('V=0.811','V=1.62','V=2.48','V=3.69','V=5.98','V=11.00','V=13.38','V=15.56','V=16.09');
 hold on;
figure(k+2)
plot(X,Y,'LineWidth',2);
grid on;
title('Projectile Motion for Fertilizer Particle');
xlabel('Horizontal Distance (m)');
ylabel('Vertical Distance (m)');
```

```
legend('V=0.811','V=1.62','V=2.48','V=3.69','V=5.98','V=11.00','V=13.38','V=15.56'
,'V=16.09');
      hold on;
      figure(k+3)
      plot(time_range,X,'LineWidth',2);
      grid on;
      title('Projectile Motion for Fertilizer Particle');
      xlabel('Time (s)');
      ylabel('Horizontal Distance (m)');

legend('V=0.811','V=1.62','V=2.48','V=3.69','V=5.98','V=11.00','V=13.38','V=15.56'
,'V=16.09');
      hold on;
      figure(k+4)
      plot(time_range,Y,'LineWidth',2);
      grid on;
      title('Projectile Motion for Fertilizer Particle');
      xlabel('Time (s)');
      ylabel('Vertical Distance (m)');

legend('V=0.811','V=1.62','V=2.48','V=3.69','V=5.98','V=11.00','V=13.38','V=15.56'
,'V=16.09');
      hold on;


   end


 end

      hold on;
```

Appendix D

```
%% Change in theta and ploting on same graph
% v = [16.09];


 %initial velocity, m/s
 v=16.09;

g = 9.8;% m/sec^2
h = 2; %initial height is 3m
% theta = (0:5:45)*(pi/180); % angle in radians
theta=[0:pi/36:pi/4];
dt=0.01;

t_total = zeros(length(v), length(theta));
Tmax = zeros(length(v), length(theta));
```

```
H_max = zeros(length(v), length(theta));
Range = zeros(length(v), length(theta));
% t_total = zeros(length(v));
% Tmax = zeros(length(v));
% Range = zeros(length(v));
% H_max = zeros(length(v));
% for ii=1:length(v)
% t_total=
 k = 1;

format short g;
for jj = 1:length(theta)
   for ii = 1:length(v)
      figure(k);
      t_total(jj,ii) = (v(ii)*sin(theta(jj))+sqrt((v(ii)*sin(theta(jj)))^2 + (2*g*h)))/g;
%Time of flight: t = [Vy + ?(Vy² + 2 * g * h)] / g
      Tmax(jj,ii) = v(ii)*sin(theta(jj))/g;%time for maximum height
      vx = v(ii)*cos(theta(jj)); % Velocity in X-Direction Vx = V * cos(?)
      vy_initial = v(ii)*sin(theta(jj));%initial velocity on launch Vy = V * sin(?)
      time_range = (0:0.01:t_total(jj,ii)); % Time Span
      if time_range(end) ~= t_total(jj,ii)
         time_range(end+1) = t_total(jj,ii);
      end
      % Total of Projectile motion

      vy = vy_initial-(g*time_range); % Velocity of fertilizer parrticle when starts to
move ertical velocity can be expressed as Vy – g * t.

      vy_final = vy_initial-(g*t_total(jj,ii)); % Velocity when fertilizer particle hit the
ground ertical velocity can be expressed as Vy – g * t.

      Y = h + (vy_initial*time_range) - 0.5*(g*time_range.^2); %Vertical distance
from the ground is described by the formula y = h + Vy * t – g * t² / 2, where g is the
gravity

      Y = round(Y*100000)/100000;

      X = vx*time_range; %Horizontal distance traveled can be expressed as x = Vx
* t, where t is the time.

      V = sqrt(vy.^2+vx.^2); %c = ?(b²+a²)
      H_max(jj,ii) = ((vy_initial^2)/(2*g))+ h;% total vertical distance, initial height
is h hmax = h + Vy² / (2 * g)
      Range(jj,ii) = vx*t_total(jj,ii) ; %Total hotizontal distance

      figure(k)
      plot(X,Y,'LineWidth',2);
      hold on;
      grid on;
      title('Projectile Motion at Different angles with same Velocity');
      xlabel('Horizontal Distance (m)');
      ylabel('Vertical Distance (m)');
```

```
legend('Theta=0','Theta=5','Theta=10','Theta=15','Theta=20','Theta=25','Theta=30','T
heta=35','Theta=40','Theta=45');
      figure(k+1)
      plot(time_range,X,'LineWidth',2);

      title('Horizontal Distance vs Time at Different Angles');
      hold on;
      grid on;
      xlabel('Time (s)');
      ylabel('Horizontal Distance (m)');

legend('Theta=0','Theta=5','Theta=10','Theta=15','Theta=20','Theta=25','Theta=30','T
heta=35','Theta=40','Theta=45');
      figure(k+2)
      plot(time_range,Y,'LineWidth',2);

      title('Vertical Distance vs Time at Different Angles');
      hold on;
      grid on;
      xlabel('Time (s)');
      ylabel('Vertical Distance (m)');

legend('Theta=0','Theta=5','Theta=10','Theta=15','Theta=20','Theta=25','Theta=30','T
heta=35','Theta=40','Theta=45');

   end

end

      hold on;


clear ii; clear jj;


 %initial velocity, m/s
 v=[16.09];

g = 9.8;% m/sec^2
h =2; %initial height is 3m
% theta = (0:5:45)*(pi/180); % angle in radians
theta=pi/6;
dt=0.01;

t_total = zeros(length(v), length(theta));
Tmax = zeros(length(v), length(theta));
H_max = zeros(length(v), length(theta));
Range = zeros(length(v), length(theta));
% t_total = zeros(length(v));
% Tmax = zeros(length(v));
% Range = zeros(length(v));
% H_max = zeros(length(v));
```

```
% for ii=1:length(v)
% t_total=
k = 1;

format short g;
for jj = 1:length(v)
    for ii = 1:length(theta)

        t_total(jj,ii) = (v(jj)*sin(theta(ii))+sqrt((v(jj)*sin(theta(ii)))^2 + (2*g*h)))/g;
        Tmax(jj,ii) = v(ii)*sin(theta(ii))/g;%time for maximum height
        vx = v(jj)*cos(theta(ii)); % Velocity in X-Direction Vx = V * cos(?)
        vy_initial = v(jj)*sin(theta(ii));%initial velocity on launch Vy = V * sin(?)
        time_range = (0:0.01:t_total(jj,ii)); % Time Span
        if time_range(end) ~= t_total(jj,ii)
            time_range(end+1) = t_total(jj,ii);
        end
        % Total of Projectile motion

        vy = vy_initial-(g*time_range); % Velocity of fertilizer parrticle when starts to
move ertical velocity can be expressed as Vy – g * t.

        vy_final = vy_initial-(g*t_total(jj,ii)); % Velocity when fertilizer particle hit the
ground ertical velocity can be expressed as Vy – g * t.

        Y = h + (vy_initial*time_range) - 0.5*(g*time_range.^2); %Vertical distance
from the ground is described by the formula y = h + Vy * t – g * t² / 2, where g is the
gravity

        Y = round(Y*100000)/100000;

        X = vx*time_range; %Horizontal distance traveled can be expressed as x = Vx
* t, where t is the time.
        V = sqrt(vy.^2+vx.^2); %c = ?(b²+a²)
        H_max(jj,ii) = ((vy_initial^2)/(2*g))+ h;% total vertical distance, initial height
is h hmax = h + Vy² / (2 * g)
        Range(jj,ii) = vx*t_total(jj,ii) ; %Total hotizontal distance
        sz=size(time_range);
        a= ones(sz);
        vx=vx*a;
        figure(k)
        plot(time_range,vx,'LineWidth',2);
        grid on;
        title('Projectile Motion for Fertilizer Particle');
        xlabel('Time (s)');
        ylabel('horizontal velocity');

legend('V=0.811','V=1.62','V=2.48','V=3.69','V=5.98','V=11.00','V=13.38','V=15.56'
,'V=16.09');
         hold on;
        figure(k+1)
        plot(time_range,vy,'LineWidth',2);
        grid on;
        title('Projectile Motion for Fertilizer Particle');
```

```
        xlabel('Time (s)');
        ylabel('vertical velocity');

legend('V=0.811','V=1.62','V=2.48','V=3.69','V=5.98','V=11.00','V=13.38','V=15.56'
,'V=16.09');
         hold on;
        figure(k+2)
        plot(X,Y,'LineWidth',2);
        grid on;
        title('Projectile Motion for Fertilizer Particle');
        xlabel('Horizontal Distance (m)');
        ylabel('Vertical Distance (m)');

legend('V=0.811','V=1.62','V=2.48','V=3.69','V=5.98','V=11.00','V=13.38','V=15.56'
,'V=16.09');
        hold on;
        figure(k+3)
        plot(time_range,X,'LineWidth',2);
        grid on;
        title('Projectile Motion for Fertilizer Particle');
        xlabel('Time (s)');
        ylabel('Horizontal Distance (m)');

legend('V=0.811','V=1.62','V=2.48','V=3.69','V=5.98','V=11.00','V=13.38','V=15.56'
,'V=16.09');
        hold on;
        figure(k+4)
        plot(time_range,Y,'LineWidth',2);
        grid on;
        title('Projectile Motion for Fertilizer Particle');
        xlabel('Time (s)');
        ylabel('Vertical Distance (m)');

legend('V=0.811','V=1.62','V=2.48','V=3.69','V=5.98','V=11.00','V=13.38','V=15.56'
,'V=16.09');
        hold on;


    end


 end

        hold on;


clear ii; clear jj;
```

Appendix E

```
%% Position of Particle in x and Y At different velocity and Same angle WITHOUT
DRAG on different figues.
%
% v = [0.811578102 1.623156204 2.486843883 3.688849066 5.982279689
%      11.00439294 13.38506684 15.56845134 16.09223616 ];


 %initial velocity, m/s
 v = [16.09];

g = 9.81;% m/sec^2
hi = 2; %initial height is 2m
theta = (0:5:45)*(pi/180); % angle in radians
dt = 0.01;

t_total = zeros(length(v), length(theta));
Tmax = zeros(length(v), length(theta));
H_max = zeros(length(v), length(theta));
range = zeros(length(v), length(theta));
% t_total = zeros(length(v));
% Tmax = zeros(length(v));
% Range = zeros(length(v));
% H_max = zeros(length(v));
% for ii=1:length(v)
% t_total=

format short g;
for jj = 1:length(v)
    for ii = 1:length(theta)

    t_total(jj,ii) = (v(jj)*sin(theta(ii))+sqrt((v(jj)*sin(theta(ii)))^2 + (2*g*hi)))/g;
%Time of flight: t = [Vy + ?(Vy² + 2 * g * h)] / g
    Tmax(jj,ii) = v(jj)*sin(theta(ii))/g;%time for maximum height
    vx = v(jj)*cos(theta(ii)); % Velocity in X-Direction Vx = V * cos(?)
    vy_initial = v(jj)*sin(theta(ii));%initial velocity on launch Vy = V * sin(?)
    time_range = (0:0.01:t_total(jj,ii)); % Time Span
    if time_range(end) ~= t_total(jj,ii)
       time_range(end+1) = t_total(jj,ii);
    end
    % Total of Projectile motion

    vy = vy_initial-(g*time_range); % Velocity of fertilizer parrticle when starts to
move ertical velocity can be expressed as Vy – g * t.

    vy_final = vy_initial-(g*t_total(jj,ii)); % Velocity when fertilizer particle hit the
ground ertical velocity can be expressed as Vy – g * t.
```

```
        Y = hi + (vy_initial*time_range) - 0.5*(g*time_range.^2); %Vertical distance from the ground is described by the formula y = h + Vy * t – g * t² / 2, where g is the gravity

        Y = round(Y*100000)/100000;

        X = vx*time_range; %Horizontal distance traveled can be expressed as x = Vx * t, where t is the time

        V = sqrt(vy.^2+vx.^2); %c = ?(b²+a²)
        H_max(jj,ii) = ((vy_initial^2)/(2*g))+ hi;% total vertical distance, initial height is h hmax = h + Vy² / (2 * g)
        range(jj,ii) = vx*t_total(jj,ii) ; %Total hotizontal distance
        end
end

clear ii; clear jj;

input_theta = input('Give me the value of angle for which you want to calculate ranges\n');
y = find(theta==(input_theta*(pi/180)));
k = 1;

figure(k);


for iii = 1 : size(range,1)
    time_range = (0:0.01:t_total(iii,y));
    vx = v(iii)*cos(input_theta*(pi/180));
    RANGE = vx*time_range;
    vy_initial = v(iii)*sin(input_theta*(pi/180));
    HEIGHT = hi + (vy_initial*time_range) - 0.5*(g*time_range.^2);
    HEIGHT = round(HEIGHT*100000)/100000;
    %legendinfo{iii} = ['Velocity = ' num2str(v(iii))];
    plot(RANGE,HEIGHT,'LineWidth',2);
end

hold on;
k = k+1;
clear iii;

figure(k);


for iii = 1 : size(range,1)
    time_range = (0:0.01:t_total(iii,y));
    vx = v(iii)*cos(input_theta*(pi/180));
    X = vx*time_range;
    %legendinfo{iii} = ['Velocity = ' num2str(v(iii))];
    plot(time_range,X,'LineWidth',2);
end

%legend(legendinfo);
```

```
hold on;
k = k+1;

clear iii;

figure(k);


for iii = 1 : size(range,1)
   time_range = (0:0.01:t_total(iii,y));
   vy_initial = v(iii)*sin(input_theta*(pi/180));
   Y = hi + (vy_initial*time_range) - 0.5*(g*time_range.^2);
   Y = round(Y*100000)/100000;
   %legendinfo{iii} = ['Velocity = ' num2str(v(iii))];
   plot(time_range,Y,'LineWidth',2);
end

%legend(legendinfo);
hold on;
k = k+1;

clear iii;
```

Appendix F

```
%% With Constant Drag Projectile Motion

Dp = 0.002;
denp = 2000;
mp = (denp*pi*Dp^3)/6;
X = [];
Y = [];
dt = .01;
g = 9.81; % m/s^2
k=1;
figure(k);

% Test whether ball has hit the ground
% ****x and y position**** 30
for j = 1:length(v)
   i = 1;
   t = [];
   t(i) = 0;
   X(j,i) = 0;
   Y(j,i) = 0 + hi;
   Vo = v(j); % m/s
   Vx = Vo*cos(input_theta*(pi/180));
   Vy = Vo*sin(input_theta*(pi/180));
   while ((Y(j,i)>0) || (i==1))
      kx = mp/((0.3*dena(6)*pi*Dp^2*Vx)/8);
```

```
        ky = mp/((0.3*dena(6)*pi*Dp^2*Vy)/8);
        t(i+1) = t(i)+dt;
        X(j,i+1) = (1/kx)*Vx*(1-exp(-kx*t(i+1)));
        Y(j,i+1) = (((1/ky)*(Vy+(g/ky))*(1-exp(-ky*t(i+1))))-(g*t(i+1)/ky)) + hi;
        i = i+1;
    end
    plot(X(j,:),Y(j,:),'LineWidth',2);

end
%{
Plot Path of Ball
 axis([0,12,0,3.5])
    title('Fertilizer Particle Path With Constant Air Drag')

    xlabel('Distance (m)')
    ylabel('Height (m)')

legend(legendinfo);
%}

hold on;
k = k+1;

% Display the max height and distance
fprintf('Max Distance = %-5.1f m\n',max(RANGE));
fprintf('Max Height = %-5.1f m\n',max(HEIGHT));
CdRange = X;
CdHeight = Y;
%% With Constant Drag Distance with time

Dp = 0.002;
denp = 2000;
mp = (denp*pi*Dp^3)/6;
dt = .01;
g = 9.81; % m/s^2
figure(k);

% Test whether ball has hit the ground
% ****x and y position**** 30
for j = 1:length(v)
    i = 1;
    t = [];
    t(i) = 0;
    X = [];
    Y = [];
    X(i) = 0;
    Y(i) = 0 + hi;
    Vo = v(j); % m/s
    Vx = Vo*cos(input_theta*(pi/180));
    Vy = Vo*sin(input_theta*(pi/180));
    while ((Y(i)>0) || (i==1))
        kx = mp/((Cd(1,6)*dena(6)*pi*Dp^2*Vx)/8);
        ky = mp/((Cd(1,6)*dena(6)*pi*Dp^2*Vy)/8);
```

```
        t(i+1) = t(i)+dt;
        X(i+1) = (1/kx)*Vx*(1-exp(-kx*t(i+1)));
        Y(i+1) = (((1/ky)*(Vy+(g/ky))*(1-exp(-ky*t(i+1))))-(g*t(i+1)/ky)) + hi;
        i = i+1;
    end
    plot(t,X,'LineWidth',2);

end

%{
 title('Fertilizer Particle Distance vs Time at Different Velocities')
axis([0,3.5,0,45])
xlabel('Time (sec)')
ylabel('Distance (m)')
legend(legendinfo);
%}
hold on;
k = k+1;

%% With Constant Drag Height with time

Dp = 0.002;
denp = 2000;
mp = (denp*pi*Dp^3)/6;
dt = .01;
g = 9.81; % m/s^2
figure(k);

% Test whether ball has hit the ground
% ****x and y position**** 30
for j = 1:length(v)
    i = 1;
    t = [];
    t(i) = 0;
    Y = [];
    Y(i) = 0 + hi;
    Vo = v(j); % m/s
    Vy = Vo*sin(input_theta*(pi/180));
    while ((Y(i)>0) || (i==1))
        ky = ((Cd(1,6)*dena(6)*pi*Dp^2*Vy)/8)/mp;
        t(i+1) = t(i)+dt;
        Y(i+1) = (((1/ky)*(Vy+(g/ky))*(1-exp(-ky*t(i+1))))-(g*t(i+1)/ky)) + hi;
        i = i+1;
    end
    plot(t,Y,'LineWidth',2);
    %legendinfo{j} = ['Velocity = ' num2str(v(j))];
end
% Plot Path of Ball
%{
title('Fertilizer Particle Height vs Time at Different Velocities');
axis([0,2.5,0,7]);
xlabel('Time (sec)');
ylabel('Height (m)');
```

```
legend(legendinfo);
%}
hold on;
k = k+1;
```

Appendix G

```
%% Description: This program plots the curve of a Fertilizer
% with variable drag force using the method of central differences.

%Define constants and variables
%Define constants and variables
Cdh = Cd(1,1); %Drag Coefficient for Reynolds Number <= 90000
Cdl = 0.1; %Drag Coefficient for Reynolds Number > 90000
g = 9.81; %Definition of gravity (m/s^2)
dt = 0.01; %Differential time step definition (s)
d = 0.002;
denp = 2000;
m = (denp*pi*d^3)/6; %mass
w = m*g; % weight (N)
p = 1.184; %Air density (kg/m^3)
mu = 1.849*10^(-5); %Viscosity of air
tau = m/(3*mu*pi*d); %Time constant (sec)

X = [];
Y = [];
T = [];

for j = 1:length(v)
i = 1; %Index
y1max = 0; %Maximum height
x1max = 0; %Maximum distance
%Define arrays
x1 = []; %Distance array
y1 = []; %Height array
u1 = []; %Horizontal velocity component array
v1 = []; %Vertical velocity component array
t = []; %Time array (sec)
%Initialize constants and variables
x1(i) = eps; %Distance initialization (m)
y1(i) =0.950+eps; %Height initialization (m)
Vo = v(j); % m/s
u1(i) = Vo*cos(input_theta*(pi/180));%Horizontal velocity component
v1(i) = Vo*sin(input_theta*(pi/180));%Vertical velocity component
Reu = eps; %Horizontal Reynolds Number
Rev = eps; %Vertical Reynolds Number
t(i) = eps; %Time initialization (sec)
% calculations
      while y1(i)>=eps
```

```
            i = i+1; %Increment the counter
            Reu = (p*d*u1(i-1))/(mu); %Define Re in the x-direction
            Rev = (p*d*v1(i-1))/(mu); %Define Re in the y-direction
            %The calculation of velocity
            if Reu > (90000) %When Re is > 90,000, the drag constant is 0.1
            u1(i)=((u1(i-1))*((48*tau)-(Cdl*Reu*dt)))/((48*tau)+(Cdl*Reu*dt));
            else %When Re is <= 90,000, the drag constant is 0.4
            u1(i)=((u1(i-1))*((48*tau)-(Cdh*Reu*dt)))/((48*tau)+(Cdh*Reu*dt));
            end
            if Rev > (90000) %When Re is > 90,000, the drag constant is 0.1
            v1(i)=((v1(i-1)*(48*tau-Cdl*Rev*dt))-
(48*tau*g*dt))/(48*tau+Cdl*Rev*dt);
            else %When Re is <= 90,000, the drag constant is 0.4
            v1(i)=((v1(i-1)*(48*tau-Cdh*Rev*dt))-
(48*tau*g*dt))/(48*tau+Cdh*Rev*dt);
            end
            %The calcualtion of position
            x1(i) = x1(i-1)+(dt/2)*(u1(i-1)+u1(i)); %Defines x-position
            y1(i) = y1(i-1)+(dt/2)*(v1(i-1)+v1(i)); %Defines y-position
            t(i) =(i-1)*dt; %Increments the time
            %Find the maximum distance and height
            if y1(i)>y1max
            y1max = y1(i);
            end
            if x1(i)>x1max
            x1max = x1(i);
            end
        end
        index(j) = length(t);

        if j>=2
        Diff_X = index(j) - index(j-1);
        X(1:j,[end+1 : end+Diff_X]) = 0;
        Diff_Y = index(j) - index(j-1);
        Y(1:j,[end+1 : end+Diff_Y]) = 0;
        Diff_T = index(j) - index(j-1);
        T(1:j,[end+1 : end+Diff_T]) = 0;
        end

        X(j,:) = 2.1*x1;
        Y(j,:) = 2.1*y1;
        T(j,:) = t;
end
% %Print the results
% fprintf('Max Distance with non-constant drag = %-5.2f m\n', x1max);
% fprintf('Max Height with non-constant drag = %-5.2f m\n', y1max);
k=1;
figure(k);

for i = 1:length(v)
plot(X(i,1:index(i)),Y(i,1:index(i)),'LineWidth',2);
end
%{
```

```
title('Horizontal Distance vs Verticle Distance with Variable air Drag');
xlabel('Horizontal Distance(m)');
ylabel('Vertical Distance(m)');
axis([0,42,0,20]);
%}


k = k+1;

figure(k)

for i = 1:length(v)
plot(T(i,1:index(i)),X(i,1:index(i)),'LineWidth',2);
end
%{
title('Plot of Range vs Time');
xlabel('Time (sec)');
ylabel('Horizontal Distance (m)');
axis([0,2.5,0,45])
%}


k = k+1;

figure(k);

for i = 1:length(v)
plot(T(i,1:index(i)),Y(i,1:index(i)),'LineWidth',2);
end
%{
title('Plot of Range vs Time');
xlabel('Time (sec)');
ylabel('Vertical Distance (m)');
axis([0,2.5,0,16])
%}

k = k+1;


clear i;
```

Appendix H

```
%%   Thrust of Drones

w = 25; % Total Weight of Drones in kg

w1 = w*9.81; % Total Weight of Dornes in Newton

p = 6; % Totoal number of propller
```

```
th = w1/p; % thrust of one Propller

% Density of Air at 25 oc

dena25 = 1.18; %kg/m3

d = 21; % Diameter in inches
d1 = (d*25.4)/1000; % Diameter in m


A = (pi*d1^2)/4; % Area of Propeller in meter
Diap = 0.0020; % In meter
%%  Description: This program plots the curve of a Fertilizer
% with variable drag force Thrust downwash using the method of central
differences.

%Define constants and variables
%Define constants and variables
k=1;
Cdh = Cd(1,1); %Drag Coefficient for Reynolds Number <= 90000
Cdl = 0.1; %Drag Coefficient for Reynolds Number > 90000
g = 9.81; %Definition of gravity (m/s^2)
dt = 0.01; %Differential time step definition (s)
d = 0.002;
denp = 2000;
m = (denp*pi*d^3)/6; %mass
w = m*g; % weight (N)
p = 1.184; %Air density (kg/m^3)
mu = 1.849*10^(-5); %Viscosity of air
tau = m/(3*mu*pi*d); %Time constant (sec)

X = [];
Y = [];
T = [];

for j = 1:length(v)
i = 1; %Index
y1max = 0; %Maximum height
x1max = 0; %Maximum distance
%Define arrays
x1 = []; %Distance array
y1 = []; %Height array
u1 = []; %Horizontal velocity component array
v1 = []; %Vertical velocity component array
t = []; %Time array (sec)
%Initialize constants and variables
x1(i) = eps; %Distance initialization (m)
y1(i) = 0.950 + eps; %Height initialization (m)
Vo = v(j); % m/s
u1(i) = Vo*cos(input_theta*(pi/180));%Horizontal velocity component
v1(i) = Vo*sin(input_theta*(pi/180));%Vertical velocity component
Reu = eps; %Horizontal Reynolds Number
```

```
Rev = eps; %Vertical Reynolds Number
t(i) = eps; %Time initialization (sec)
% calculations
      while y1(i)>=eps
            i = i+1; %Increment the counter
            Reu = (p*d*u1(i-1))/(mu); %Define Re in the x-direction
            Rev = (p*d*v1(i-1))/(mu); %Define Re in the y-direction
            %The calculation of velocity
            if Reu > (90000) %When Re is > 90,000, the drag constant is 0.1
            u1(i)=((u1(i-1))*((48*tau)-(Cdl*Reu*dt)))/((48*tau)+(Cdl*Reu*dt));
            else %When Re is <= 90,000, the drag constant is 0.4
            u1(i)=((u1(i-1))*((48*tau)-(Cdh*Reu*dt)))/((48*tau)+(Cdh*Reu*dt));
            end
            if Rev > (90000) %When Re is > 90,000, the drag constant is 0.1
            v1(i)=((v1(i-1)*(48*tau-Cdl*Rev*dt))-
(48*tau*g*dt))/(48*tau+Cdl*Rev*dt);
            else %When Re is <= 90,000, the drag constant is 0.4
            v1(i)=((v1(i-1)*(48*tau-Cdh*Rev*dt))-
(48*tau*g*dt))/(48*tau+Cdh*Rev*dt);
            end



            %The calcualtion of position
            x1(i) = x1(i-1)+(dt/2)*(u1(i-1)+u1(i)); %Defines x-position
            %The downwash
            if x1(i) < 1.00
               v1(i) = v1(i) - dt*(0.5*Cd*dena25*Ap*(vair)^2)/m;
               downaccel= 0.5*Cd*dena25*Ap*(vair)^2;
            end




            y1(i) = y1(i-1)+(dt/2)*(v1(i-1)+v1(i)); %Defines y-position
            t(i) =(i-1)*dt; %Increments the time
            %Find the maximum distance and height
            if y1(i)>y1max
            y1max = y1(i);
            end
            if x1(i)>x1max
            x1max = x1(i);
            end
       end
      index(j) = length(t);

      if j>=2
      Diff_X = index(j) - index(j-1);
      X(1:j,[end+1 : end+Diff_X]) = 0;
      Diff_Y = index(j) - index(j-1);
      Y(1:j,[end+1 : end+Diff_Y]) = 0;
      Diff_T = index(j) - index(j-1);
      T(1:j,[end+1 : end+Diff_T]) = 0;
```

```
    end

    X(j,:) = 2.1*x1;
    Y(j,:) = 2.1*y1;
    T(j,:) = t;
end
% %Print the results
% fprintf('Max Distance with non-constant drag = %-5.2f m\n', x1max);
% fprintf('Max Height with non-constant drag = %-5.2f m\n', y1max);
figure(k);

for i = 1:length(v)
plot(X(i,1:index(i)),Y(i,1:index(i)),'LineWidth',2);
end
title('Horizontal Distance vs Vertical Distance at V=16.09')
xlabel('Horizontal Distance (m)');
ylabel('Vertical Distance (m)');
ylim([0 7])
legend ('No Air Drag','Constant Drag','Variable Air Drag','DownWash Air Thrust')
%{
title('Plot of Trajectory');
xlabel('Horizontal Distance(m)');
ylabel('Vertical Distance(m)');
axis([0,50,0,20]);
legend ('Air Drag Is Funcation of Speed')
%}
hold on
k = k+1;

figure(k)

for i = 1:length(v)
plot(T(i,1:index(i)),X(i,1:index(i)),'LineWidth',2);
end
title('Horiontal Distance vs Time at V=16.09');
xlabel('Time (sec)');
ylabel('Horizontal Distance (m)');
legend ('No Air Drag','Constant Drag','Variable Air Drag','DownWash Air Thrust')
%{
title('Plot of Range vs Time');
xlabel('Time (sec)');
ylabel('Horizontal Distance (m)');
axis([0,4,0,50])
legend ('Air Drag Is Funcation of Speed')
hold off
%}
hold on;
k = k+1;

figure(k);

for i = 1:length(v)
plot(T(i,1:index(i)),Y(i,1:index(i)),'LineWidth',2);
```

```
end
title('Vertical Distance vs Time at V=16.09');
xlabel('Time (sec)');
ylabel('Vertical Distance (m)');
legend ('No Air Drag','Constant Drag','Variable Air Drag','DownWash Air Thrust')
%{
title('Plot of Range vs Time');
xlabel('Time (sec)');
ylabel('Vertical Distance (m)');

legend ('Air Drag Is Funcation of Speed')
hold off
%}
hold on;
k = k+1;


clear i;
```

References

[1] S. Ahmad, “AGRICULTURAL PAKISTAN REPORT Secretary,” 2010.

[2] T. P. Minister and A. T. Plan, “Agricultural Survey of Pakistan 2020-21”.

[3] P. P. Patil, A. Subhashrao Ghodke, S. R. Kalme, M. Ashish, and R. Devshette, “Urea Spreader Machine,” *Int. Res. J. Eng. Technol.*, p. 2345, 2019.

[4] FAO, *Food Outlook*, no. October. 2022.

[5] Government of Pakistan, “02-Agriculture Economic survey 20 21,” 2021.

[6] Chandini, R. Kumar, R. Kumar, and O. Prakash, “The Impact of Chemical Fertilizers on our Environment and Ecosystem,” *Res. Trends Environ. Sci.*, 2019.

[7] S. Savci, “An Agricultural Pollutant: Chemical Fertilizer,” *Int. J. Environ. Sci. Dev.*, 2012, doi: 10.7763/ijesd.2012.v3.191.

[8] J. Cooper *et al.*, “Phosphorus availability on many organically managed farms in Europe,” *Nutr. Cycl. Agroecosystems*, 2018, doi: 10.1007/s10705-017-9894-2.

[9] A. Sharma, “A Review on the Effect of Organic and Chemical Fertilizers on Plants,” *Int. J. Res. Appl. Sci. Eng. Technol.*, 2017, doi: 10.22214/ijraset.2017.2103.

[10] P. Heffer, “Assessment of Fertilizer Use by Crop at the Global Level,” *Int. Fertil. Ind. Assoc.*, vol. 5, no. 8, p. 9, 2013.

[11] FAO, *World fertilizer outlook and trends to 2022*. 2019.

[12] D. P. ASTUTI, *No Title העינים לנגד שבאמת מה את לראות קשה הכי*, no. 8.5.2017. 2022.

[13] H. González-Jorge, J. Martínez-Sánchez, M. Bueno, and P. Arias, "Unmanned Aerial Systems for Civil Applications: A Review," 2017, doi: 10.3390/drones1010002.

[14] N. Vargas-Ramírez and J. Paneque-Gálvez, "drones The Global Emergence of Community Drones," 2012, doi: 10.3390/drones3040076.

[15] "Long Range Fixed-wing VTOL Drone | 2 Hours Endurance." https://www.yangdaonline.com/yangda-fw-250-fixed-wing-vtol-plane/ (accessed Aug. 18, 2022).

[16] "Global Multi Rotor Drone Market, Multi Rotor Drone Industry, Multi Rotor Drone Market Research Report - Ken Research." https://www.kenresearch.com/blog/2020/02/global-multi-rotor-drone-market/ (accessed Aug. 18, 2022).

[17] D. Pattern, "Granular Pesticided Distrbution pattern from a helicopter-borne Spreader," 1997.

[18] D. Chen and G. X. Gao, "Probabilistic graphical fusion of LiDAR, GPS, and 3D building maps for urban UAV navigation," *Navig. J. Inst. Navig.*, vol. 66, no. 1, pp. 151–168, 2019, doi: 10.1002/navi.298.

[19] H. Nawaz, H. M. Ali, and S.-R. Massan, "Applications of unmanned aerial vehicles: a review," *3C Tecnol. innovación Apl. a la pyme*, no. November, pp. 85–105, 2019, doi: 10.17993/3ctecno.2019.specialissue3.85-105.

[20] F. Garcia-Ruiz, S. Sankaran, J. M. Maja, W. S. Lee, J. Rasmussen, and R. Ehsani, "Comparison of two aerial imaging platforms for identification of Huanglongbing-infected citrus trees," *Comput. Electron. Agric.*, vol. 91, pp. 106–115, 2013, doi: 10.1016/j.compag.2012.12.002.

[21] C. Zhang and J. M. Kovacs, "The application of small unmanned aerial systems for precision agriculture: A review," *Precision Agriculture*. 2012. doi: 10.1007/s11119-012-9274-5.

[22] Z. Lu, F. Nagata, and K. Watanabe, "Development of iOS application handlers for quadrotor UAV remote control and monitoring," *2017 IEEE Int. Conf. Mechatronics Autom. ICMA 2017*, pp. 513–518, 2017, doi: 10.1109/ICMA.2017.8015870.

[23] M. Cheng *et al.*, “Estimation of soil moisture content under high maize canopy coverage from UAV multimodal data and machine learning,” *Agric. Water Manag.*, vol. 264, no. February, p. 107530, 2022, doi: 10.1016/j.agwat.2022.107530.

[24] W. Wu, M. A. Qurishee, J. Owino, I. Fomunung, M. Onyango, and B. Atolagbe, “Coupling Deep Learning and UAV for Infrastructure Condition Assessment Automation,” *2018 IEEE Int. Smart Cities Conf. ISC2 2018*, pp. 1–7, 2019, doi: 10.1109/ISC2.2018.8656971.

[25] J. Cuaran and J. Leon, “Crop Monitoring using Unmanned Aerial Vehicles: A Review,” *Agric. Rev.*, no. Of, 2021, doi: 10.18805/ag.r-180.

[26] M. A. Jiménez-Bello, A. Royuela, J. Manzano, P. J. Zarco-Tejada, and D. Intrigliolo, “Assessment of drip irrigation sub-units using airborne thermal imagery acquired with an Unmanned Aerial Vehicle (UAV) BT - Precision agriculture ’13,” 2013, pp. 705–711.

[27] A. C. Watts, V. G. Ambrosia, and E. A. Hinkley, “Unmanned aircraft systems in remote sensing and scientific research: Classification and considerations of use,” *Remote Sens.*, vol. 4, no. 6, pp. 1671–1692, 2012, doi: 10.3390/rs4061671.

[28] Think Defence, “Black Hornet Nano UAV,” pp. 20–24, 2013.

[29] M. Keennon and J. Grasmeyer, “Development of Two MAVs and Vision of the Future of MAV Design,” in *AIAA International Air and Space Symposium and Exposition: The Next 100 Years*, doi: 10.2514/6.2003-2901.

[30] A. Type, “Aeryon Skyranger R60,” pp. 1–8.

[31] R. All and A. A. Cookies, “Puma ™ 3 ae,” pp. 1–10.

[32] T. Boeing and I. Scaneagle, “Boeing Insitu ScanEagle - Wikipedia,” pp. 1–16, 2005.

[33] N. Tv, “Ikhana / Predator B Unmanned Aerial Vehicle,” pp. 21–23.

[34] P. Station, “The first stratospheric UAS of its kind.” pp. 1–12.

[35] C. Y. N. Norasma, M. A. Fadzilah, N. A. Roslin, Z. W. N. Zanariah, Z. Tarmidi, and F. S. Candra, “Unmanned Aerial Vehicle Applications in Agriculture,” *IOP Conf. Ser. Mater. Sci. Eng.*, vol. 506, no. 1, 2019, doi: 10.1088/1757-899X/506/1/012063.

[36] I. Zambon, M. Cecchini, G. Egidi, M. G. Saporito, and A. Colantoni, “Revolution 4.0: Industry vs. agriculture in a future development for SMEs,” *Processes*, vol. 7, no. 1, 2019, doi: 10.3390/pr7010036.

[37] D. J. Mulla, “Twenty five years of remote sensing in precision agriculture: Key advances and remaining knowledge gaps,” *Biosyst. Eng.*, vol. 114, no. 4, pp. 358–371, 2013, doi: 10.1016/j.biosystemseng.2012.08.009.

[38] W. H. Maes and K. Steppe, “Perspectives for Remote Sensing with Unmanned Aerial Vehicles in Precision Agriculture,” *Trends Plant Sci.*, vol. 24, no. 2, pp. 152–164, 2019, doi: 10.1016/j.tplants.2018.11.007.

[39] P. Radoglou-grammatikis, P. Sarigiannidis, and T. Lagkas, “A compilation of UAV applications for precision agriculture,” *Comput. Networks*, vol. 172, no. February, p. 107148, 2020, doi: 10.1016/j.comnet.2020.107148.

[40] J. Albetis *et al.*, “Detection of Flavescence dorée grapevine disease using Unmanned Aerial Vehicle (UAV) multispectral imagery,” *Remote Sens.*, vol. 9, no. 4, pp. 1–20, 2017, doi: 10.3390/rs9040308.

[41] “Fixed Wing UAV | 3D CAD Model Library | GrabCAD.” https://grabcad.com/library/fixed-wing-uav-3 (accessed Aug. 27, 2022).

[42] “HammerHead Electric Vtol | Technosys Embedded Systems.” https://www.technosysind.com/hammerhead-electric-vtol-drone-uav/ (accessed Aug. 27, 2022).

[43] J. W. Hofstee and W. Huisman, “Handling and spreading of fertilizers part 1: Physical properties of fertilizer in relation to particle motion,” *J. Agric. Eng. Res.*, vol. 47, no. C, pp. 213–234, 1990, doi: 10.1016/0021-8634(90)80043-T.

[44] H. T. Sogaard and P. Kierkegaard, “Yield Reduction Resulting from Uneven Fertilizer Distribution,” *Trans. ASAE*, vol. 37, no. 6, pp. 1749–1752, 1994, doi: 10.13031/2013.28262.

[45] R. Horrell, A. K. Metherell, S. Ford, and C. Doscher, “Fertilizer evenness - losses and costs: A study on the economic benefits of uniform applications of fertilizer,” *Proc. New Zeal. Grassl. Assoc.*, pp. 215–220, Jan. 1999, doi: 10.33584/JNZG.1999.61.2337.

[46] R. Olieslagers, H. Ramon, and J. De Baerdemaeker, “Calculation of fertilizer distribution patterns from a spinning disc spreader by means of a simulation model,” *J. Agric. Eng. Res.*, vol. 63, no. 2, pp. 137–152, 1996, doi: 10.1006/jaer.1996.0016.

[47] R. Reints and R. Yoerger, “TRAJECTORIES OF SEEDS AND GRANULAR FERTILIZERS,” *undefined*, vol. 10, no. 2, pp. 0213–0216, 1967, doi: 10.13031/2013.39637.

[48] R. J. Atkin, W. D. Collins, and P. E. Rawlins, “How does air resistance affect the motion of a projectile?,” *Teach. Math. its Appl.*, vol. 12, no. 2, pp. 78–82, 1993, doi: 10.1093/teamat/12.2.78.

[49] C. Information, “Reynolds number,” *SpringerReference*, no. October 2019, pp. 2–3, 2011, doi: 10.1007/springerreference_30449.

[50] S. A. Morsi and A. J. Alexander, “An investigation of particle trajectories in two-phase flow systems,” *J. Fluid Mech.*, vol. 55, no. 2, pp. 193–208, Sep. 1972, doi: 10.1017/S0022112072001806.

[51] A. R. KHAN and J. F. RICHARDSON, “THE RESISTANCE TO MOTION OF A SOLID SPHERE IN A FLUID,” *Chem. Eng. Commun.*, vol. 62, no. 1–6, pp. 135–150, 1987, doi: 10.1080/00986448708912056.

[52] R. L. C. Flemmer and C. L. Banks, “On the drag coefficient of a sphere,” *Powder Technol.*, vol. 48, no. 3, pp. 217–221, Nov. 1986, doi: 10.1016/0032-5910(86)80044-4.

[53] R. Turton and O. Levenspiel, “A short note on the drag correlation for spheres,” *Powder Technol.*, vol. 47, no. 1, pp. 83–86, 1986, doi: 10.1016/0032-5910(86)80012-2.

[54] A. Haider and O. Levenspiel, “Drag coefficient and terminal velocity of spherical and nonspherical particles,” *Powder Technol.*, vol. 58, no. 1, pp. 63–70, May 1989, doi: 10.1016/0032-5910(89)80008-7.

[55] D. Pattern, “Pesticide from helicopter-borne,” 2007.

[56] A. Alaimo, V. Artale, C. L. R. Milazzo, and A. Ricciardello, “PID controller applied to hexacopter flight,” *J. Intell. Robot. Syst. Theory Appl.*, vol. 73, no. 1–4, pp. 261–270, 2014, doi: 10.1007/S10846-013-9947-Y.

[57] V. Artale, C. L. R. Milazzo, and A. Ricciardello, “Mathematical modeling of hexacopter,” *Appl. Math. Sci.*, vol. 7, no. 97–100, pp. 4805–4811, 2013, doi: 10.12988/AMS.2013.37385.

[58] C. Morales, D. Ovalle, and A. Gauthier, “Hexacopter maneuverability capability: An optimal control approach,” *2017 7th Int. Conf. Model. Simulation, Appl. Optim. ICMSAO 2017*, May 2017, doi: 10.1109/ICMSAO.2017.7934920.

[59] Z. Wu *et al.*, “Simulation and parameter optimisation of a centrifugal rice seeding spreader for a UAV,” *Biosyst. Eng.*, 2020, doi: 10.1016/j.biosystemseng.2020.02.004.

[60] M. F.Daqaq, *Dynamics of Particle and Rigid Bodies*, vol. 44, no. 8. 2019. doi: 10.1088/1751-8113/44/8/085201.

[61] T. Asai and K. Seo, “Aerodynamic drag of modern soccer balls,” *Springerplus*, vol. 2, no. 1, pp. 2–6, 2013, doi: 10.1186/2193-1801-2-171.

[62] J. E. Goff and M. J. Carré, “Trajectory analysis of a soccer ball,” *Am. J. Phys.*, vol. 77, no. 11, pp. 1020–1027, 2009, doi: 10.1119/1.3197187.

[63] K. Bray and D. G. Kerwin, “Modelling the flight of a soccer ball in a direct free kick,” *J. Sports Sci.*, vol. 21, no. 2, pp. 75–85, 2003, doi: 10.1080/0264041031000070994.

CERTIFICATE OF COMPLETENESS

It is hereby certified that the dissertation submitted by NS Muhammad Zubair, Reg No.

00000117387, Titled: ***Design and Development of Aerial Fertilizer Spreader for improved Efficiency.***has been checked/reviewed and its contents are complete in all respects.

Supervisor's Name: **Dr. Imran Akhtar** Signature: _____

Date: _____